Robust linearly constrained extended Kalman filter for mismatched nonlinear systems

Emir Hrustic, Rayen Ben Abdallah, Jordi Vilà-valls, Damien Vivet, Gaël Pagès, Eric Chaumette

DOI: 10.1002/rnc.5305

RESEARCH ARTICLE

Robust linearly constrained extended Kalman filter for mismatched nonlinear systems

Emir Hrustic | **Rayen Ben Abdallah** | **Jordi Vilà-Valls** | **Damien Vivet** | **Gaël Pagès** | **Eric Chaumette**

ISAE-SUPAERO, University of Toulouse, Toulouse, France

Correspondence
Jordi Vilà-Valls, ISAE-SUPAERO, University of Toulouse, Toulouse, France.
Email: jordi.vila-valls@isae-supaero.fr

Funding information
Agence Nationale de la Recherche, Grant/Award Number: ANR-17-CE22-0001-01; Délégation Générale pour l'Armement, Grant/Award Numbers: 2018.60.0072.00.470.75.01, 2019.65.0068.00.470.75.01

Summary
Standard state estimation techniques, ranging from the linear Kalman filter (KF) to nonlinear extended KF (EKF), sigma-point or particle filters, assume a perfectly known system model, that is, process and measurement functions and system noise statistics (both the distribution and its parameters). This is a strong assumption which may not hold in practice, reason why several approaches have been proposed for robust filtering, mainly because the filter performance is particularly sensitive to different model mismatches. In the context of linear filtering, a solution to cope with possible system matrices mismatch is to use linear constraints. In this contribution we further explore the extension and use of recent results on linearly constrained KF for robust nonlinear filtering under both process and measurement model mismatch. We first investigate how linear equality constraints can be incorporated within the EKF and derive a new linearly constrained extended KF (LCEKF). Then we detail its use to mitigate parametric modeling errors in the nonlinear process and measurement functions. Numerical results are provided to show the performance improvement of the new LCEKF for robust vehicle navigation.

KEYWORDS
linearly constrained extended Kalman filter, model mismatch, robust filtering, robust vehicle navigation

1 | INTRODUCTION

It is well known that state estimation (ie, infer the dynamic states of a system from a set of available noisy observations) is a fundamental task in robotics, tracking, guidance, and navigation systems, to name a few[1-4]. In general, either if the state-space representation of the system dynamics is linear or nonlinear, standard state estimation techniques assume a perfect knowledge of the system characteristics, which may not be a reasonable assumption in real-life applications. For linear dynamic systems, the best linear minimum mean square error (MSE) estimator is given by the Kalman filter (KF).[5] In this case, the main assumptions are perfectly known system matrices, known noise first and second-order statistics, and perfect initialization. The same limitations apply to the popular extended KF (EKF),[5] the family of sigma-point filters,[6,7] or sequential Monte Carlo methods,[8] for which a perfect knowledge of nonlinear process and measurement functions and both noise statistics must be considered. That is the reason why there exists a continued effort to develop robust filtering techniques. Among them, a lot of effort has been devoted to the mitigation of nonnominal/unknown

noise behaviors/parameters: (i) estimating the Gaussian noise covariances,[9,10] (ii) considering heavy-tailed distributions together with variational Bayesian approximations[11-13] or exploiting conjugate analysis,[14] or (iii) relying in fundamental results arising in robust statistics to counteract the presence of outliers.[15-17] By contrast, few contributions explored how to counteract a mismatch on system matrices or the filter initialization.

Within the KF framework the latter can be solved with distortionless constraints.[18,19] If the state dynamics representation is unknown, a possible solution is to use several filters running in parallel with different process models via the so-called interacting multiple model filter.[20] A fundamentally different approach is to use linear equality constraints in order to mitigate a process and/or measurement model matrices mismatch. How to incorporate nonstationary constraints within the KF framework has been recently proposed in Reference 21, leading to a general linearly constrained KF (LCKF) formulation, which has been shown in Reference 22 for linear systems to generalize the results in Reference 23.

For nonlinear systems, the EKF is one of the most popular estimation techniques and therefore has been largely investigated.[1,3,24] The sensitivity of the EKF to the filter initialization and its inevitable divergence if the noise matrices have not been chosen appropriately, together with the analysis of the related stability and robustness of the filter, has been widely reported in the open literature.[25,26] The EKF performance also depends on the accurate knowledge of the observation parametric model (linear or nonlinear system functions) and is particularly sensitive to different types of mismatches between the assumed signal model and the real signal.[27,28] Thus, in order to provide additional robustness to modeling errors, state constraints may be introduced, yielding the so-called constrained EKF (CEKF).[29,30] Recently, the CEKF has attracted a lot of attention and the use of state constraints has increased in practical engineering applications such as robotics,[31] navigation,[32] as well as target tracking.[33] The use of linear equality constraints in nonlinear systems has been briefly explored in [23, section IV] where the Unscented KF is applied to the gain-constrained linear KF, which in turn is a particular instance of the LCKF.[21,22] But the analysis in Reference 23 only applies the linear constrained gain computation with the unscented innovation covariance approximation, and no further discussion is provided. Moreover, this approach is not intended to be a robust filtering solution under model mismatch. As previously stated,[21] recently proposed a different approach where linear constraints (LCs) are used to mitigate process and/or measurement model matrices mismatch in linear systems. The use of constraints for robust filtering under model mismatch in nonlinear systems has not been yet explored, thus being an important missing point.

In this contribution we further explore the extension and applicability of the LCKF to mitigate possible process and/or measurement model mismatch in nonlinear dynamic systems. The main contributions are: (i) we investigate how linear equality constraints can be incorporated within the EKF, (ii) we derive a new linearly constrained EKF (LCEKF), (iii) we detail the use of constraints to mitigate parametric modeling errors in the nonlinear process and measurement functions, and (iv) we show the performance improvement in the context of robust vehicle navigation.

The article is organized as follows: Section 2 provides background result on KF, model mismatch and LCKF; The new LCEKF is derived in Section 3, together with its use to mitigate parametric modeling errors in the nonlinear system functions, and the extension of these results to the mismatched inputs case; The details on both the three-wheeled vehicle dynamic and measurement models are given in Section 4; The application of the new LCEKF for robust vehicle navigation is illustrated in Section 5; Finally, conclusions and remarks are drawn in Section 6.

The following notations are adopted along this article: italic indicates a scalar quantity, lower case boldface indicates a vector quantity and upper case boldface a matrix. The operator $\mathbb{E}[.]$ denotes the expectation operator, the filter estimates based on measurements up to and including time k is denoted by $\hat{\mathbf{x}}_{k|k}$ and $\mathcal{N}(\boldsymbol{\mu}, \mathbf{R})$ is the normal distribution of mean $\boldsymbol{\mu}$ and covariance matrix $\mathbf{R}$, $\mathbf{m}_{\mathbf{z}}$ denotes the mean value of a given variable $\mathbf{z}$ and the $\overline{\mathbf{z}}_n$ denotes the vectorization of the set $\{\mathbf{z}_n\}$ as $\overline{\mathbf{z}}_n = (\mathbf{z}_1^T, \mathbf{z}_2^T, \ldots, \mathbf{z}_n^T)^T$.

2 | BACKGROUND ON WIENER, KALMAN, MODEL MISMATCH AND LCKF

2.1 | Wiener and Kalman

Given $\mathbf{x}$ and $\mathbf{y}$ two complex random vectors, the linear estimator of $\mathbf{x}$ which minimizes the MSE is the so-called (affine) Wiener filter (WF)[1,2]

[1]The superscript $(\cdot)^b$ stands for the best solution in the MSE sense.

$$\hat{\mathbf{x}}^b(\mathbf{y}) = \mathbf{K}^b\mathbf{y} + \mathbf{a}^b = \mathbf{m}_\mathbf{x} + \mathbf{K}^b(\mathbf{y} - \mathbf{m}_\mathbf{y}), \tag{1a}$$

$$(\mathbf{K}^b, \mathbf{a}^b) = \arg\min_{(\mathbf{K},\mathbf{a})} \{\mathbf{P}(\mathbf{K}, \mathbf{a}))\},\ \mathbf{P}(\mathbf{K}, \mathbf{a}) = \mathbb{E}[(\mathbf{K}\mathbf{y} + \mathbf{a} - \mathbf{x})(\mathbf{K}\mathbf{y} + \mathbf{a} - \mathbf{x})^H],$$

$$\mathbf{K}^b = \mathbf{C}_{\mathbf{x},\mathbf{y}}\mathbf{C}_\mathbf{y}^{-1}, \quad \mathbf{a}^b = \mathbf{m}_\mathbf{x} - \mathbf{K}^b\mathbf{m}_\mathbf{y}, \quad \mathbf{P}(\mathbf{K}^b, \mathbf{a}^b) = \mathbf{C}_{\mathbf{x}|\mathbf{y}} = \mathbf{C}_\mathbf{x} - \mathbf{C}_{\mathbf{x},\mathbf{y}}\mathbf{C}_\mathbf{y}^{-1}\mathbf{C}_{\mathbf{x},\mathbf{y}}^H,$$

considering that $\mathbf{C}_\mathbf{y}$ is invertible, with $\mathbf{C}_\mathbf{x}$, $\mathbf{C}_\mathbf{y}$, $\mathbf{C}_{\mathbf{x},\mathbf{y}}$, $\mathbf{C}_{\mathbf{x}|\mathbf{y}}$ the corresponding covariance, crosscovariance, and conditional covariance matrices, $\mathbf{m}_\mathbf{x} = \mathbb{E}[\mathbf{x}]$ and $\mathbf{m}_\mathbf{y} = \mathbb{E}[\mathbf{y}]$. If we consider a linear discrete state-space model (SSM), where the state $\mathbf{x}_k \in \mathbb{C}^{P_k}$ must be estimated from available measurements $\mathbf{y}_k \in \mathbb{C}^{N_k}$ (for $k \geq 1$): $\mathbf{x}_k = \mathbf{F}_{k-1}\mathbf{x}_{k-1} + \mathbf{w}_{k-1}$ and $\mathbf{y}_k = \mathbf{H}_k\mathbf{x}_k + \mathbf{v}_k$; with $\mathbf{F}_{k-1} \in \mathbb{C}^{P_k \times P_{k-1}}$ and $\mathbf{H}_k \in \mathbb{C}^{N_k \times P_k}$ known system model (process and measurement) matrices, $\mathbf{w}_k \in \mathbb{C}^{P_k}$ and $\mathbf{v}_k \in \mathbb{C}^{N_k}$ the process and measurement noise with known mean and covariance, then the WF estimate of $\mathbf{x}_k$ from measurements up to time k is

$$\hat{\mathbf{x}}_{k|k}^b = \mathbf{m}_{\mathbf{x}_k} + \mathbb{K}_k^b(\overline{\mathbf{y}}_k - \mathbf{m}_{\overline{\mathbf{y}}_k})\ ;\ \mathbb{K}_k^b = \mathbf{C}_{\mathbf{x}_k,\overline{\mathbf{y}}_k}\mathbf{C}_{\overline{\mathbf{y}}_k}^{-1}, \tag{2}$$

where $\overline{\mathbf{y}}_k^\top = [\mathbf{y}_1^\top, \ldots, \mathbf{y}_k^\top]$. Obviously this formulation is not useful in practice due to its computational complexity increase with k, thus a recursive form must be obtained. If a minimum set of uncorrelation conditions hold[18] then (2) can be expressed in a recursive predictor/corrector form (for $k \geq 1$), which is a general KF form,

$$\hat{\mathbf{x}}_{k|k-1}^b = \mathbf{F}_{k-1}\hat{\mathbf{x}}_{k-1|k-1}^b + \mathbf{m}_{\mathbf{w}_{k-1}}\ ;\ \hat{\mathbf{y}}_{k|k-1}^b = \mathbf{H}_k\hat{\mathbf{x}}_{k|k-1}^b + \mathbf{m}_{\mathbf{v}_k}, \tag{3a}$$

$$\hat{\mathbf{x}}_{k|k}^b = \hat{\mathbf{x}}_{k|k-1}^b + \mathbf{K}_k^b(\mathbf{y}_k - \hat{\mathbf{y}}_{k|k-1}^b), \tag{3b}$$

where the corresponding prediction/estimation error covariance matrices and optimal gain are given by

$$\mathbf{P}_{k|k-1}^b = \mathbf{F}_{k-1}\mathbf{P}_{k-1|k-1}^b\mathbf{F}_{k-1}^H + \mathbf{C}_{\mathbf{w}_{k-1}} + \mathbf{F}_{k-1}\mathbf{C}_{\mathbf{w}_{k-1},\mathbf{x}_{k-1}}^H + \mathbf{C}_{\mathbf{w}_{k-1},\mathbf{x}_{k-1}}\mathbf{F}_{k-1}^H \tag{4a}$$

$$\mathbf{K}_k^b = (\mathbf{P}_{k|k-1}^b\mathbf{H}_k^H + \mathbf{C}_{\mathbf{v}_k,\mathbf{x}_k}^H)(\mathbf{S}_{k|k-1}^b)^{-1}\ ;\ \mathbf{S}_{k|k-1}^b = \mathbf{H}_k\mathbf{P}_{k|k-1}^b\mathbf{H}_k^H + \mathbf{C}_{\mathbf{v}_k} + \mathbf{H}_k\mathbf{C}_{\mathbf{v}_k,\mathbf{x}_k}^H + \mathbf{C}_{\mathbf{v}_k,\mathbf{x}_k}\mathbf{H}_k^H \tag{4b}$$

$$\mathbf{P}_{k|k}^b = (\mathbf{I} - \mathbf{K}_k^b\mathbf{H}_k)\mathbf{P}_{k|k-1}^b - \mathbf{K}_k^b\mathbf{C}_{\mathbf{v}_k,\mathbf{x}_k}, \tag{4c}$$

with $\mathbf{P}_{0|0}^b = \mathbf{C}_{\mathbf{x}_0}$ and $\hat{\mathbf{x}}_{0|0}^b = \mathbb{E}[\mathbf{x}_0]$. Notice that the standard KF equations[3] are obtained if both system noises are zero-mean, uncorrelated with the state and among them.

2.2 | Model mismatch in linear SSM

In the previous derivations the main assumptions are: (i) known system matrices $\mathbf{F}_k$ and $\mathbf{H}_k$, (ii) known first- and second-order process and measurement noise statistics, $\mathbf{m}_{\mathbf{w}_k}$, $\mathbf{m}_{\mathbf{v}_k}$, $\mathbf{C}_{\mathbf{w}_k}$, $\mathbf{C}_{\mathbf{v}_k}$, and (iii) perfect initialization, $\mathbf{P}_{0|0}^b = \mathbf{C}_{\mathbf{x}_0}$ and $\hat{\mathbf{x}}_{0|0}^b = \mathbb{E}[\mathbf{x}_0]$. However, in real-life applications we may have to cope with the SSM pair

$$\text{Mismatched SSM } \begin{cases} \mathbf{x}_k' = \hat{\mathbf{F}}_{k-1}\mathbf{x}_{k-1}' + \mathbf{w}_{k-1} \\ \mathbf{y}_k = \hat{\mathbf{H}}_k\mathbf{x}_k' + \mathbf{v}_k \end{cases} \tag{5a}$$

$$\text{True SSM } \begin{cases} \mathbf{x}_k = \mathbf{F}_{k-1}\mathbf{x}_{k-1} + \mathbf{w}_{k-1} \\ \mathbf{y}_k = \mathbf{H}_k\mathbf{x}_k + \mathbf{v}_k \end{cases} \tag{5b}$$

modeling the fact that our assumed knowledge of the system dynamics (5a) introduces a possible mismatch between the true matrices, $\mathbf{F}_k$, $\mathbf{H}_k$ and the assumed ones, $\hat{\mathbf{F}}_k$ and $\hat{\mathbf{H}}_k$,

$$\mathbf{F}_k = \hat{\mathbf{F}}_k + d\mathbf{F}_k\ ;\ \mathbf{H}_k = \hat{\mathbf{H}}_k + d\mathbf{H}_k. \tag{6}$$

Since it is known for ages that the performance of WF and KF strongly depends on the accurate knowledge on system matrices [34-36, section 6.6], the ultimate goal in robust filtering is still to estimate accurately the true state $\mathbf{x}_k$ based on the (true) measurements $\mathbf{y}_k$ despite a misspecification of $\mathbf{F}_k$ and $\mathbf{H}_k$. Indeed, it has been recently shown analytically that a system model mismatch induces an estimation bias and MSE performance loss.[37]

2.3 | Linearly constrained KF

In order to robustify the WF several contributions have studied the use of LCs, leading to the so-called linearly constrained WF (LCWF) [36, section 6.6, 2,28]. The family of LCs which allows to reformulate the LCWF in a recursive form, leading to a general LCKF, has been analyzed in Reference 21. In Reference 21, it has also been shown that LCs can be used to mitigate a misspecification of $\mathbf{F}_k$ and $\mathbf{H}_k$. We summarize the LCKF formulation in the sequel. Introducing a set of LCs $\mathbb{K}_k\overline{\mathbf{\Lambda}}_k = \mathbf{T}_k$ in the WF problem (2) (ie, for centered $\mathbf{x}_k$ and $\mathbf{y}_k$) yields the following LCWF,

$$\hat{\mathbf{x}}^b_{k|k} = \mathbb{L}^b_k\overline{\mathbf{y}}_k, \tag{7a}$$

$$\mathbb{L}^b_k = \arg\min_{\mathbb{L}_k}\{\mathbf{P}_{k|k}(\mathbb{L}_k)\} \text{ s.t. } \mathbb{L}_k\overline{\mathbf{\Lambda}}_k = \mathbf{T}_k, \tag{7b}$$

$$\mathbb{L}^b_k = \mathbb{K}^b_k + (\mathbf{T}_k - \mathbb{K}^b_k\overline{\mathbf{\Lambda}}_k)(\overline{\mathbf{\Lambda}}^H_k\mathbf{C}^{-1}_{\overline{\mathbf{y}}_k}\overline{\mathbf{\Lambda}}_k)^{-1}\overline{\mathbf{\Lambda}}^H_k\mathbf{C}^{-1}_{\overline{\mathbf{y}}_k}.$$

It is possible to obtain a recursive LCWF estimate of $\mathbf{x}_k$[21]

$$\hat{\mathbf{x}}^b_{k|k} = \hat{\mathbf{x}}_{k|k}(\mathbf{L}^b_k) = (\mathbf{I} - \mathbf{L}^b_k\mathbf{H}_k)\mathbf{F}_{k-1}\hat{\mathbf{x}}^b_{k-1|k-1} + \mathbf{L}^b_k\mathbf{y}_k, \tag{8}$$

$$\hat{\mathbf{x}}_{k|k}(\mathbf{L}_k) = (\mathbf{I} - \mathbf{L}_k\mathbf{H}_k)\mathbf{F}_{k-1}\hat{\mathbf{x}}^b_{k-1|k-1} + \mathbf{L}_k\mathbf{y}_k, \tag{9}$$

where at every time k, $k \geq 1$, the gain $\mathbf{L}^b_k$ is given by

$$\mathbf{L}^b_k = \arg\min_{\mathbf{L}_k}\{\mathbf{P}^J_{k|k}(\mathbf{L}_k)\} \text{ s.t. } \mathbf{L}_k\mathbf{\Delta}_k = \mathbf{T}_k, \tag{10}$$

$$\mathbf{P}^J_{k|k}(\mathbf{L}_k) = \mathbb{E}[(\hat{\mathbf{x}}_{k|k}(\mathbf{L}_k) - \mathbf{x}_k)(\hat{\mathbf{x}}_{k|k}(\mathbf{L}_k) - \mathbf{x}_k)^H], \tag{11}$$

with $\mathbf{L}_k\mathbf{\Delta}_k = \mathbf{T}_k$ a set of LCs, and computed from the following "constrained" KF recursion

$$\mathbf{P}^b_{k|k-1} = \mathbf{F}_{k-1}\mathbf{P}^b_{k-1|k-1}\mathbf{F}^H_{k-1} + \mathbf{C}_{\mathbf{w}_{k-1}} + \mathbf{F}_{k-1}\mathbf{C}^H_{\mathbf{w}_{k-1},\mathbf{x}_{k-1}} + \mathbf{C}_{\mathbf{w}_{k-1},\mathbf{x}_{k-1}}\mathbf{F}^H_{k-1} \tag{12a}$$

$$\mathbf{S}^b_{k|k-1} = \mathbf{H}_k\mathbf{P}^b_{k|k-1}\mathbf{H}^H_k + \mathbf{C}_{\mathbf{v}_k} + \mathbf{H}_k\mathbf{C}_{\mathbf{x}_k,\mathbf{v}_k} + \mathbf{C}_{\mathbf{v}_k,\mathbf{x}_k}\mathbf{H}^H_k \tag{12b}$$

$$\mathbf{K}_k = \left(\mathbf{P}^b_{k|k-1}\mathbf{H}^H_k + \mathbf{C}^H_{\mathbf{v}_k,\mathbf{x}_k}\right)\left(\mathbf{S}^b_{k|k-1}\right)^{-1} \tag{12c}$$

$$\mathbf{L}^b_k = \mathbf{K}_k + \mathbf{\Gamma}_k\mathbf{\Psi}^{-1}_k\mathbf{\Delta}^H_k\left(\mathbf{S}^b_{k|k-1}\right)^{-1} \tag{12d}$$

$$\mathbf{P}^b_{k|k} = (\mathbf{I} - \mathbf{K}_k\mathbf{H}_k)\mathbf{P}^b_{k|k-1} - \mathbf{K}_k\mathbf{C}_{\mathbf{v}_k,\mathbf{x}_k} + \mathbf{\Gamma}_k\mathbf{\Psi}^{-1}_k\mathbf{\Gamma}^H_k \tag{12e}$$

with $\mathbf{\Gamma}_k = \mathbf{T}_k - \mathbf{K}_k\mathbf{\Delta}_k$ and $\mathbf{\Psi}_k = \mathbf{\Delta}^H_k(\mathbf{S}^b_{k|k-1})^{-1}\mathbf{\Delta}_k$. Notice that $\mathbf{K}_k$ is the unconstrained KF gain. Such recursive LCWF (so-called LCKF) is fully adaptive and allows to incorporate or not new LCs at every k. In case that at a given time no LCs are considered, the gain is obtained from the unconstrained KF recursion (4b). In terms of computational complexity, notice that the only difference between the KF and the LCKF is on the Kalman gain computation, which includes the LCs. Therefore, the marginal computational complexity increase (w.r.t. the std KF and the computation of $\mathbf{K}_k$) is only an additional matrix multiplication $\mathbf{L}^b_k = \mathbf{K}_k + \mathbf{\Gamma}_k\mathbf{\Psi}^{-1}_k\mathbf{\Delta}^H_k(\mathbf{S}^b_{k|k-1})^{-1}$, where $(\mathbf{S}^b_{k|k-1})^{-1}$ is readily available from the standard gain computation, $\mathbf{K}_k = (\mathbf{P}^b_{k|k-1}\mathbf{H}^H_k + \mathbf{C}^H_{\mathbf{v}_k,\mathbf{x}_k})(\mathbf{S}^b_{k|k-1})^{-1}$. Therefore, the LCKF can be used in any real-life application where the KF is already applied.

2.4 | Error mitigation in linear SSMs with mismatched process and measurement matrices

At time $k \geq 1$, the KF of $\mathbf{x}_k$ is obtained from the Kalman recursion (3b) to (4c) computed with the mismatched SSM (5a)

$$\hat{\mathbf{x}}^b_{k|k-1} = \hat{\mathbf{F}}_{k-1}\hat{\mathbf{x}}^b_{k-1|k-1} + \mathbf{m}_{\mathbf{w}_{k-1}} \; ; \; \hat{\mathbf{y}}^b_{k|k-1} = \hat{\mathbf{H}}_k\hat{\mathbf{x}}^b_{k|k-1} + \mathbf{m}_{\mathbf{v}_k},$$
$$\hat{\mathbf{x}}_{k|k}(\mathbf{L}_k) = \hat{\mathbf{x}}^b_{k|k-1} + \mathbf{L}_k(\mathbf{y}_k - \hat{\mathbf{y}}^b_{k|k-1}),$$

where $\mathbf{L}_k \triangleq \mathbf{L}^b_k$ is the solution of $\mathbf{L}^b_k = \arg\min_{\mathbf{L}_k} \left\{\mathbf{P}^J_{k|k}(\mathbf{L}_k)\right\}$. However, because of the measurement matrix mismatch, the estimation error introduced by the KF recursion above is

$$\hat{\mathbf{x}}_{k|k}(\mathbf{L}_k) - \mathbf{x}_k = (\mathbf{I} - \mathbf{L}_k\hat{\mathbf{H}}_k)(\hat{\mathbf{F}}_{k-1}(\hat{\mathbf{x}}^b_{k-1|k-1} - \mathbf{x}_{k-1}) - \mathbf{w}_{k-1}) + \mathbf{L}_k\mathbf{v}_k + \boldsymbol{\epsilon}_k(\mathbf{L}_k), \tag{13a}$$

$$\boldsymbol{\epsilon}_k(\mathbf{L}_k) = \mathbf{L}_k d\mathbf{H}_k\mathbf{x}_k - (\mathbf{I} - \mathbf{L}_k\hat{\mathbf{H}}_k)d\mathbf{F}_{k-1}\mathbf{x}_{k-1}, \tag{13b}$$

where $\boldsymbol{\epsilon}_k(\mathbf{L}_k)$ is the error term induced by the model mismatch (ie, $\boldsymbol{\epsilon}_k(\mathbf{L}_k) = \mathbf{0}$ if $\hat{\mathbf{F}}_k = \mathbf{F}_k$ and $\hat{\mathbf{H}}_k = \mathbf{H}_k$). This extra term is not taken into account in the Kalman gain computation (4a) to (4c) and induces an estimation bias and MSE performance loss.[37] Thus, in order to mitigate the impact of such mismatch, at every time step we can force $\boldsymbol{\epsilon}_k(\mathbf{L}_k) = \mathbf{0}$, which translates to the following LCs,

$$\{\mathbf{L}_k d\mathbf{H}_k = \mathbf{0}, \; (\mathbf{I} - \mathbf{L}_k\hat{\mathbf{H}}_k)d\mathbf{F}_{k-1} = \mathbf{0}\}. \tag{14a}$$

Notice that these LCs provide a nondegenerate solution only if $rank(d\mathbf{F}_{k-1}) = R_k < P_k$. In this case, (14a) can be recast as

$$\{\mathbf{L}_k d\mathbf{H}_k = \mathbf{0}, \; \mathbf{L}_k(\hat{\mathbf{H}}_k d\mathbf{F}_{k-1}) = d\mathbf{F}_{k-1}\}. \tag{14b}$$

More specifically, let $d\mathbf{F}_{k-1} = \mathbf{U}_{k-1}d\boldsymbol{\Phi}_{k-1}$ be the singular value decomposition of $d\mathbf{F}_{k-1}$, where $\mathbf{U}_{k-1} \in \mathbb{C}^{P_k \times R_k}$ has full rank $R_k < P_k$ and $d\boldsymbol{\Phi}_{k-1} \in \mathbb{C}^{R_k \times P_{k-1}}$.[38] Then (14a) becomes

$$\{\mathbf{L}_k d\mathbf{H}_k = \mathbf{0}, \; \mathbf{L}_k(\hat{\mathbf{H}}_k\mathbf{U}_{k-1}) = \mathbf{U}_{k-1}\}. \tag{14c}$$

By imposing these LCs the estimate obtained with the mismatched SSM (5a) is matched to the true observation (5b). Indeed, then (13a) reduces to

$$\hat{\mathbf{x}}_{k|k}(\mathbf{L}_k) - \mathbf{x}_k = (\mathbf{I} - \mathbf{L}_k\hat{\mathbf{H}}_k)(\hat{\mathbf{F}}_{k-1}(\hat{\mathbf{x}}^b_{k-1|k-1} - \mathbf{x}_{k-1}) - \mathbf{w}_{k-1}) + \mathbf{L}_k\mathbf{v}_k,$$

and the LCKF minimizes the MSE associated to the true state $\mathbf{x}_k$, matching the true observations to the assumed model.

3 | A NEW LCEKF AND ITS USE IN ROBUST FILTERING

3.1 | Standard EKF

If we consider now a nonlinear discrete SSM,

$$\mathbf{x}_k = \mathbf{f}_{k-1}(\mathbf{x}_{k-1}) + \mathbf{w}_{k-1} = \mathbf{f}_{k-1}(\mathbf{x}_{k-1}) + \mathbf{m}_{\mathbf{w}_{k-1}} + d\mathbf{w}_{k-1}, \tag{15a}$$

$$\mathbf{y}_k = \mathbf{h}_k(\mathbf{x}_k) + \mathbf{v}_k = \mathbf{h}_k(\mathbf{x}_k) + \mathbf{m}_{\mathbf{v}_k} + d\mathbf{v}_k, \tag{15b}$$

with $\mathbf{f}_{k-1}(\cdot)$ and $\mathbf{h}_k(\cdot)$ known system model (process and measurement) functions, and $\mathbb{E}[d\mathbf{w}_{k-1}] = \mathbf{0}$, $\mathbb{E}[d\mathbf{v}_k] = \mathbf{0}$. A standard approach to derive a nonlinear filter of $\mathbf{x}_k$ is to assume that the nonlinear discrete SSM (15a) and (15b) can be

linearized at the vicinity of a so-called nominal trajectory[3] yielding the so-called linearized KF, as follows. If we assume that: (i) $tr(\mathbf{C}_{\mathbf{x}_0}) \ll 1$ (small deviations of the initial state from its mean value), (ii) $tr(\mathbf{C}_{\mathbf{w}_{k-1}}) \ll 1$ (small state noise), and (iii) $tr(\mathbf{C}_{\mathbf{x}_{k-1}}) \ll 1$ (small deviations of the states from their mean value), then one can resort to a first-order Taylor expansion of $\mathbf{f}_{k-1}(\mathbf{x}_{k-1})$ at the vicinity of $\mathbf{m}_{\mathbf{x}_{k-1}}$,

$$\mathbf{x}_k \simeq \mathbf{f}_{k-1}(\mathbf{m}_{\mathbf{x}_{k-1}}) + \mathbf{F}_{k-1} d\mathbf{x}_{k-1} + \mathbf{m}_{\mathbf{w}_{k-1}} + d\mathbf{w}_{k-1} \simeq \mathbf{m}_{\mathbf{x}_k} + \mathbf{F}_{k-1} d\mathbf{x}_{k-1} + d\mathbf{w}_{k-1}, \tag{16}$$

with $\mathbf{F}_{k-1} = \left.\frac{\partial \mathbf{f}_{k-1}(\mathbf{x}_{k-1})}{\partial \mathbf{x}_{k-1}^T}\right|_{\mathbf{m}_{\mathbf{x}_{k-1}}}$ and $\mathbf{m}_{\mathbf{x}_k} \simeq \mathbf{f}_{k-1}(\mathbf{m}_{\mathbf{x}_{k-1}}) + \mathbf{m}_{\mathbf{w}_{k-1}}$, and to a first-order Taylor expansion of $\mathbf{h}_k(\mathbf{x}_k)$ at the vicinity of $\mathbf{m}_{\mathbf{x}_k}$,

$$\mathbf{h}_k(\mathbf{x}_k) \simeq \mathbf{h}_k(\mathbf{m}_{\mathbf{x}_k} + \mathbf{F}_{k-1} d\mathbf{x}_{k-1} + d\mathbf{w}_{k-1}) \simeq \mathbf{h}_k(\mathbf{m}_{\mathbf{x}_k}) + \mathbf{H}_k(\mathbf{F}_{k-1} d\mathbf{x}_{k-1} + d\mathbf{w}_{k-1}), \tag{17}$$

with $\mathbf{H}_k = \left.\frac{\partial \mathbf{h}_k(\mathbf{x}_k)}{\partial \mathbf{x}_k^T}\right|_{\mathbf{m}_{\mathbf{x}_k}}$. Then (15a) and (15b) is equivalent to

$$\begin{cases} \mathbf{x}_k \simeq \mathbf{F}_{k-1}\mathbf{x}_{k-1} + \mathbf{m}_{\mathbf{w}'_{k-1}} + d\mathbf{w}'_{k-1}, \\ \mathbf{y}_k \simeq \mathbf{H}_k\mathbf{x}_k + \mathbf{m}_{\mathbf{v}'_k} + d\mathbf{v}'_k, \end{cases} \begin{cases} \mathbf{C}_{d\mathbf{w}'_{k-1}} = \mathbf{C}_{d\mathbf{w}_{k-1}} = \mathbf{C}_{\mathbf{w}_{k-1}} \\ \mathbf{m}_{\mathbf{w}'_{k-1}} = \mathbf{m}_{\mathbf{x}_k} - \mathbf{F}_{k-1}\mathbf{m}_{\mathbf{x}_{k-1}} \\ \mathbf{C}_{d\mathbf{v}'_k} = \mathbf{C}_{d\mathbf{v}_k} = \mathbf{C}_{\mathbf{v}_k} \\ \mathbf{m}_{\mathbf{v}'_k} = \mathbf{m}_{\mathbf{v}_k} + \mathbf{h}_k(\mathbf{m}_{\mathbf{x}_k}) - \mathbf{H}_k\mathbf{m}_{\mathbf{x}_k} \end{cases} \tag{18}$$

If a set of uncorrelation conditions are verified[18] ($\forall k \geq 1$), then the EKF recursion is given by

$$\hat{\mathbf{x}}^b_{k|k} = \hat{\mathbf{x}}^b_{k|k-1} + \mathbf{K}^b_k(\mathbf{y}_k - \hat{\mathbf{y}}^b_{k|k-1}), \tag{19a}$$

$$\hat{\mathbf{x}}^b_{k|k-1} \simeq \mathbf{F}_{k-1}\hat{\mathbf{x}}^b_{k-1|k-1} + \mathbf{m}_{\mathbf{w}'_{k-1}} \simeq \mathbf{f}_{k-1}(\hat{\mathbf{x}}^b_{k-1|k-1}) + \mathbf{m}_{\mathbf{w}_{k-1}}, \tag{19b}$$

$$\hat{\mathbf{y}}^b_{k|k-1} \simeq \mathbf{H}_k\hat{\mathbf{x}}^b_{k|k-1} + \mathbf{m}_{\mathbf{v}'_k} \simeq \mathbf{h}_k(\hat{\mathbf{x}}^b_{k|k-1}) + \mathbf{m}_{\mathbf{v}_k}, \tag{19c}$$

where the Kalman gain is computed as in (4b) with the corresponding linearized $\mathbf{F}_{k-1}$ and $\mathbf{H}_k$. Notice that $\mathbf{m}_{\mathbf{x}_{k-1}}$ is generally unknown. Therefore, the following last hypothesis is made: $\hat{\mathbf{x}}^b_{k-1|k-1} \simeq \mathbf{m}_{\mathbf{x}_{k-1}}$ (small deviations from the mean value) which allows to approximate $\mathbf{F}_{k-1}$ and $\mathbf{H}_k$ with,

$$\mathbf{F}_{k-1} \simeq \left.\frac{\partial \mathbf{f}_{k-1}(\boldsymbol{x}_{k-1})}{\partial \boldsymbol{x}_{k-1}^T}\right|_{\hat{\mathbf{x}}^b_{k-1|k-1}}, \mathbf{H}_k \simeq \left.\frac{\partial \mathbf{h}_k(\boldsymbol{x}_k)}{\partial \boldsymbol{x}_k^T}\right|_{\hat{\mathbf{x}}^b_{k|k-1}},$$

which complete the popular EKF recursion formulation, this last hypothesis making sense if the EKF converges (small estimation errors), since then:

$$tr(\mathbf{P}^b_{k-1|k-1}) = \mathbb{E}[\|\hat{\mathbf{x}}^b_{k-1|k-1} - \mathbf{x}_{k-1}\|^2] \ll 1.$$

3.2 | Impact of parametric modeling errors on the nonlinear state and measurement system functions

Since the EKF of $\mathbf{x}_k$ is based on the measurements and our knowledge of the model dynamics, any mismatch between the true system model and the assumed system model leads to a suboptimal filter, and possibly to a filter with bad performance, as the discrepancy between the two models increases. The existence of uncertainty on the nonlinear state and measurement functions, $\mathbf{f}_{k-1}(\cdot)$ and $\mathbf{h}_k(\cdot)$, can be illustrated by the case where a parametric model is known: $\mathbf{f}_{k-1}(.) \triangleq \mathbf{f}_{k-1}(., \boldsymbol{\omega})$ and $\mathbf{h}_k(.) \triangleq \mathbf{h}_k(., \boldsymbol{\theta})$, where $\boldsymbol{\omega}$ and $\boldsymbol{\theta}$ are supposed to be deterministic vectors determined via an ad hoc calibration process. In many cases, such calibration process provides an estimate, $\hat{\boldsymbol{\omega}} = \boldsymbol{\omega} + d\hat{\boldsymbol{\omega}}$ and $\hat{\boldsymbol{\theta}} = \boldsymbol{\theta} + d\hat{\boldsymbol{\theta}}$, of the true

values, $\boldsymbol{\omega}$ and $\boldsymbol{\theta}$. If the calibration process is accurate enough, that is, $d\hat{\boldsymbol{\omega}}$ and $d\hat{\boldsymbol{\theta}}$ are small, the true nonlinear state and measurement functions differ from the assumed ones via the following first-order Taylor series

$$\mathbf{f}_{k-1}(\mathbf{x}_{k-1}, \boldsymbol{\omega}) \simeq \mathbf{f}_{k-1}(\mathbf{x}_{k-1}, \hat{\boldsymbol{\omega}}) + \frac{\partial \mathbf{f}_{k-1}(\mathbf{x}_{k-1}, \hat{\boldsymbol{\omega}})}{\partial \boldsymbol{\omega}^T}(\boldsymbol{\omega} - \hat{\boldsymbol{\omega}}) \tag{20a}$$

$$\mathbf{h}_k(\mathbf{x}_k, \boldsymbol{\theta}) \simeq \mathbf{h}_k(\mathbf{x}_k, \hat{\boldsymbol{\theta}}) + \frac{\partial \mathbf{h}_k(\mathbf{x}_k, \hat{\boldsymbol{\theta}})}{\partial \boldsymbol{\theta}^T}(\boldsymbol{\theta} - \hat{\boldsymbol{\theta}}). \tag{20b}$$

Thus, similar to (5a) and (5b), we want to cope with the situation where there is a true and a mismatched nonlinear SSM,

$$\text{Mismatched}: \begin{cases} \mathbf{x}'_k = \mathbf{f}_{k-1}(\mathbf{x}'_{k-1}, \hat{\boldsymbol{\omega}}) + \mathbf{m}_{\mathbf{w}_{k-1}} + d\mathbf{w}_{k-1} \\ \mathbf{y}_k = \mathbf{h}_k(\mathbf{x}'_k, \hat{\boldsymbol{\theta}}) + \mathbf{m}_{\mathbf{v}_k} + d\mathbf{v}_k \end{cases} \tag{21a}$$

$$\text{True SSM}: \begin{cases} \mathbf{x}_k = \mathbf{f}_{k-1}(\mathbf{x}_{k-1}, \boldsymbol{\omega}) + \mathbf{m}_{\mathbf{w}_{k-1}} + d\mathbf{w}_{k-1} \\ \mathbf{y}_k = \mathbf{h}_k(\mathbf{x}_k, \boldsymbol{\theta}) + \mathbf{m}_{\mathbf{v}_k} + d\mathbf{v}_k \end{cases} \tag{21b}$$

At time $k \geq 1$, the EKF of $\mathbf{x}_k$ is obtained from the Kalman-like recursion (19a) to (19c) computed with the mismatched SSM

$$\hat{\mathbf{x}}^b_{k|k-1} = \mathbf{f}_{k-1}(\hat{\mathbf{x}}^b_{k-1|k-1}, \hat{\boldsymbol{\omega}}) + \mathbf{m}_{\mathbf{w}_{k-1}} \; ; \; \hat{\mathbf{y}}^b_{k|k-1} = \mathbf{h}_k(\hat{\mathbf{x}}^b_{k|k-1}, \hat{\boldsymbol{\theta}}) + \mathbf{m}_{\mathbf{v}_k}, \tag{22a}$$

$$\hat{\mathbf{x}}_{k|k}(\mathbf{L}_k) = \hat{\mathbf{x}}^b_{k|k-1} + \mathbf{L}_k(\mathbf{y}_k - \hat{\mathbf{y}}^b_{k|k-1}), \tag{22b}$$

where $\mathbf{L}_k \triangleq \mathbf{L}^b_k$ is the solution of $\mathbf{L}^b_k = \arg\min_{\mathbf{L}_k} \{\mathbf{P}^I_{k|k}(\mathbf{L}_k)\}$, computed with the mismatched SSM.

As done for the linear SSM in (13a), we can assess the impact of the parametric modeling error as

$$\begin{aligned} \hat{\mathbf{x}}_{k|k}(\mathbf{L}_k) - \mathbf{x}_k = {} & \mathbf{f}_{k-1}(\hat{\mathbf{x}}^b_{k-1|k-1}, \hat{\boldsymbol{\omega}}) - \mathbf{f}_{k-1}(\mathbf{x}_{k-1}, \hat{\boldsymbol{\omega}}) + \mathbf{L}_k \mathbf{h}_k(\mathbf{f}_{k-1}(\mathbf{x}_{k-1}, \hat{\boldsymbol{\omega}}) + \mathbf{m}_{\mathbf{w}_{k-1}} + d\mathbf{w}_{k-1}, \hat{\boldsymbol{\theta}}) \\ & - \mathbf{L}_k \mathbf{h}_k(\mathbf{f}_{k-1}(\hat{\mathbf{x}}^b_{k-1|k-1}, \hat{\boldsymbol{\omega}}) + \mathbf{m}_{\mathbf{w}_{k-1}}, \hat{\boldsymbol{\theta}}) + \mathbf{L}_k d\mathbf{v}_k - d\mathbf{w}_{k-1} + \boldsymbol{\varepsilon}_k(\mathbf{L}_k), \end{aligned} \tag{23a}$$

where the error term is

$$\boldsymbol{\varepsilon}_k(\mathbf{L}_k) = \mathbf{f}_{k-1}(\mathbf{x}_{k-1}, \hat{\boldsymbol{\omega}}) - \mathbf{f}_{k-1}(\mathbf{x}_{k-1}, \boldsymbol{\omega}) + \mathbf{L}_k \mathbf{h}_k(\mathbf{x}_k, \boldsymbol{\theta}) - \mathbf{L}_k \mathbf{h}_k(\mathbf{f}_{k-1}(\mathbf{x}_{k-1}, \hat{\boldsymbol{\omega}}) + \mathbf{m}_{\mathbf{w}_{k-1}} + d\mathbf{w}_{k-1}, \hat{\boldsymbol{\theta}}). \tag{23b}$$

Since $\mathbf{f}_k(\mathbf{x}_k)$ and $\mathbf{h}_k(\mathbf{x}_k)$ have become, respectively, $\mathbf{f}_k(\mathbf{x}_k, \boldsymbol{\omega})$ and $\mathbf{h}_k(\mathbf{x}_k, \boldsymbol{\theta})$, then: $\mathbf{m}_{\mathbf{x}_k} \simeq \mathbf{f}_{k-1}(\mathbf{m}_{\mathbf{x}_{k-1}}, \boldsymbol{\omega}) + \mathbf{m}_{\mathbf{w}_{k-1}}$, $\mathbf{F}_{k-1} = \left.\frac{\partial \mathbf{f}_{k-1}(\boldsymbol{x}_{k-1}, \boldsymbol{\omega})}{\partial \boldsymbol{x}^T_{k-1}}\right|_{\mathbf{m}_{\mathbf{x}_{k-1}}}$, $\mathbf{H}_k = \left.\frac{\partial \mathbf{h}_k(\mathbf{x}_k, \boldsymbol{\theta})}{\partial \mathbf{x}^T_k}\right|_{\mathbf{m}_{\mathbf{x}_k}}$.

Moreover, we denote: $\hat{\mathbf{m}}_{\mathbf{x}_k} \simeq \mathbf{f}_{k-1}(\mathbf{m}_{\mathbf{x}_{k-1}}, \hat{\boldsymbol{\omega}}) + \mathbf{m}_{\mathbf{w}_{k-1}}$, $\hat{\mathbf{F}}_{k-1} = \left.\frac{\partial \mathbf{f}_{k-1}(\boldsymbol{x}_{k-1}, \hat{\boldsymbol{\omega}})}{\partial \boldsymbol{x}^T_{k-1}}\right|_{\mathbf{m}_{\mathbf{x}_{k-1}}}$, $\hat{\mathbf{H}}_k = \left.\frac{\partial \mathbf{h}_k(\mathbf{x}_k, \hat{\boldsymbol{\theta}})}{\partial \mathbf{x}^T_k}\right|_{\hat{\mathbf{m}}_{\mathbf{x}_k}}$.

3.3 | On the first-order EKF error approximation

First, from the previous results we have that,

$$\mathbf{f}_{k-1}(\mathbf{x}_{k-1}, \hat{\boldsymbol{\omega}}) \simeq \mathbf{f}_{k-1}(\mathbf{m}_{\mathbf{x}_{k-1}}, \hat{\boldsymbol{\omega}}) + \hat{\mathbf{F}}_{k-1}(\mathbf{x}_{k-1} - \mathbf{m}_{\mathbf{x}_{k-1}}), \tag{24a}$$

$$\mathbf{h}_k(\mathbf{f}_{k-1}(\mathbf{x}_{k-1}, \hat{\boldsymbol{\omega}}) + \mathbf{m}_{\mathbf{w}_{k-1}} + d\mathbf{w}_{k-1}, \hat{\boldsymbol{\theta}}) \simeq \mathbf{h}_k(\hat{\mathbf{m}}_{\mathbf{x}_k}, \hat{\boldsymbol{\theta}}) + \hat{\mathbf{H}}_k \hat{\mathbf{F}}_{k-1}(\mathbf{x}_{k-1} - \mathbf{m}_{\mathbf{x}_{k-1}}) + \hat{\mathbf{H}}_k d\mathbf{w}_{k-1}. \tag{24b}$$

Second, if we assume that $\hat{\mathbf{x}}^b_{k-1|k-1}$ is a good enough unbiased estimate of $\mathbf{x}_{k-1}$, that is,

$$\mathbb{E}[\hat{\mathbf{x}}^b_{k-1|k-1}] = \mathbb{E}[\mathbf{x}_{k-1}] = \mathbf{m}_{\mathbf{x}_{k-1}}, \; tr(\mathbf{P}^b_{k-1|k-1}) = \mathbb{E}[\|\hat{\mathbf{x}}^b_{k-1|k-1} - \mathbf{x}_{k-1}\|^2] \ll 1, \tag{25a}$$

then,

$$\mathbf{f}_{k-1}(\hat{\mathbf{x}}^b_{k-1|k-1}, \hat{\boldsymbol{\omega}}) \simeq \mathbf{f}_{k-1}(\mathbf{m}_{\mathbf{x}_{k-1}}, \hat{\boldsymbol{\omega}}) + \hat{\mathbf{F}}_{k-1}(\hat{\mathbf{x}}^b_{k-1|k-1} - \mathbf{m}_{\mathbf{x}_{k-1}}), \tag{26a}$$

$$\mathbf{h}_k(\mathbf{f}_{k-1}(\hat{\mathbf{x}}^b_{k-1|k-1}, \hat{\boldsymbol{\omega}}) + \mathbf{m}_{\mathbf{w}_{k-1}}, \hat{\boldsymbol{\theta}}) \simeq \mathbf{h}_k(\hat{\mathbf{m}}_{\mathbf{x}_k}, \hat{\boldsymbol{\theta}}) + \hat{\mathbf{H}}_k\hat{\mathbf{F}}_{k-1}(\hat{\mathbf{x}}^b_{k-1|k-1} - \mathbf{m}_{\mathbf{x}_{k-1}}). \tag{26b}$$

Thus, if we assume that $\hat{\mathbf{x}}^b_{k-1|k-1}$ is a good enough unbiased estimate of $\mathbf{x}_{k-1}$, a first-order approximation of (23a) is

$$\hat{\mathbf{x}}_{k|k}(\mathbf{L}_k) - \mathbf{x}_k \simeq (\mathbf{I} - \mathbf{L}_k\hat{\mathbf{H}}_k)\hat{\mathbf{F}}_{k-1}(\hat{\mathbf{x}}^b_{k-1|k-1} - \mathbf{x}_{k-1}) - (\mathbf{I} - \mathbf{L}_k\hat{\mathbf{H}}_k)d\mathbf{w}_{k-1} + \mathbf{L}_k d\mathbf{v}_k + \boldsymbol{\varepsilon}_k(\mathbf{L}_k), \tag{27}$$

with $\boldsymbol{\varepsilon}_k(\mathbf{L}_k)$ given in (23b).

3.4 | On the first-order $\boldsymbol{\varepsilon}_k(\mathbf{L}_k)$ error term approximation

Notice that the approximation of $\mathbf{f}_{k-1}(\mathbf{x}_{k-1}, \hat{\boldsymbol{\omega}})$ is given in (24a), and $\mathbf{h}_k(\mathbf{f}_{k-1}(\mathbf{x}_{k-1}, \hat{\boldsymbol{\omega}}) + \mathbf{m}_{\mathbf{w}_{k-1}} + d\mathbf{w}_{k-1}, \hat{\boldsymbol{\theta}})$ in (24b). In addition, using (20a) and (20b), we can write that

$$\mathbf{f}_{k-1}(\mathbf{x}_{k-1}, \boldsymbol{\omega}) = \mathbf{f}_{k-1}(\mathbf{x}_{k-1}, \hat{\boldsymbol{\omega}} + (\boldsymbol{\omega} - \hat{\boldsymbol{\omega}})) \simeq \mathbf{f}_{k-1}(\mathbf{m}_{\mathbf{x}_{k-1}}, \hat{\boldsymbol{\omega}}) + \hat{\mathbf{F}}_{k-1}(\mathbf{x}_{k-1} - \mathbf{m}_{\mathbf{x}_{k-1}}) + \frac{\partial \mathbf{f}_{k-1}(\mathbf{x}_{k-1}, \hat{\boldsymbol{\omega}})}{\partial \boldsymbol{\omega}^T}(\boldsymbol{\omega} - \hat{\boldsymbol{\omega}}), \tag{28a}$$

and

$$\mathbf{h}_k(\mathbf{x}_k, \boldsymbol{\theta}) = \mathbf{h}_k(\mathbf{x}_k, \hat{\boldsymbol{\theta}} + (\boldsymbol{\theta} - \hat{\boldsymbol{\theta}})) \simeq \mathbf{h}_k(\hat{\mathbf{m}}_{\mathbf{x}_k}, \hat{\boldsymbol{\theta}}) + \hat{\mathbf{H}}_k(\hat{\mathbf{F}}_{k-1}(\mathbf{x}_{k-1} - \mathbf{m}_{\mathbf{x}_{k-1}}) + d\mathbf{w}_{k-1}) \tag{28b}$$

$$+ \hat{\mathbf{H}}_k \frac{\partial \mathbf{f}_{k-1}(\mathbf{x}_{k-1}, \hat{\boldsymbol{\omega}})}{\partial \boldsymbol{\omega}^T}(\boldsymbol{\omega} - \hat{\boldsymbol{\omega}}) + \frac{\partial \mathbf{h}_k(\mathbf{x}_k, \hat{\boldsymbol{\theta}})}{\partial \boldsymbol{\theta}^T}(\boldsymbol{\theta} - \hat{\boldsymbol{\theta}}), \tag{28c}$$

and therefore we can approximate the error term $\boldsymbol{\varepsilon}_k(\mathbf{L}_k)$ in (23b) as

$$\boldsymbol{\varepsilon}_k(\mathbf{L}_k) \simeq \mathbf{L}_k \frac{\partial \mathbf{h}_k(\mathbf{x}_k, \hat{\boldsymbol{\theta}})}{\partial \boldsymbol{\theta}^T}(\boldsymbol{\theta} - \hat{\boldsymbol{\theta}}) - (\mathbf{I} - \mathbf{L}_k\hat{\mathbf{H}}_k)\frac{\partial \mathbf{f}_{k-1}(\mathbf{x}_{k-1}, \hat{\boldsymbol{\omega}})}{\partial \boldsymbol{\omega}^T}(\boldsymbol{\omega} - \hat{\boldsymbol{\omega}}). \tag{29}$$

3.5 | Link with the mismatched KF error in (13a) and (13b)

If we assume that the nonlinear SSM model (21a) and (21b) becomes linear, we have that

$$\mathbf{f}_{k-1}(\mathbf{x}_{k-1}, \boldsymbol{\omega}) = \mathbf{F}_{k-1}(\boldsymbol{\omega})\mathbf{x}_{k-1} \; ; \; \mathbf{h}_k(\mathbf{x}_k, \boldsymbol{\theta}) = \mathbf{H}_k(\boldsymbol{\theta})\mathbf{x}_k, \tag{30a}$$

where

$$\mathbf{F}_{k-1}(\boldsymbol{\omega}) = \left[\mathbf{f}^1_{k-1}(\boldsymbol{\omega}) \; \ldots \; \mathbf{f}^{P_{k-1}}_{k-1}(\boldsymbol{\omega})\right] \; ; \; \mathbf{H}_k(\boldsymbol{\theta}) = \left[\mathbf{h}^1_k(\boldsymbol{\theta}) \; \ldots \; \mathbf{h}^{P_k}_k(\boldsymbol{\theta})\right],$$

then

$$\frac{\partial \mathbf{h}_k(\boldsymbol{x}_k, \boldsymbol{\theta})}{\partial \boldsymbol{x}^T_k} = \frac{\partial(\mathbf{H}_k(\boldsymbol{\theta})\boldsymbol{x}_k)}{\partial \boldsymbol{x}^T_k} = \mathbf{H}_k(\boldsymbol{\theta}) \; ; \; \frac{\partial \mathbf{f}_{k-1}(\boldsymbol{x}_{k-1}, \boldsymbol{\omega})}{\partial \boldsymbol{x}^T_{k-1}} = \frac{\partial(\mathbf{F}_{k-1}(\boldsymbol{\omega})\boldsymbol{x}_{k-1})}{\partial \boldsymbol{x}^T_{k-1}} = \mathbf{F}_{k-1}(\boldsymbol{\omega}),$$

leading to

$$\hat{\mathbf{H}}_k = \left.\frac{\partial \mathbf{h}_k(\mathbf{x}_k, \hat{\boldsymbol{\theta}})}{\partial \mathbf{x}^T_k}\right|_{\hat{\mathbf{m}}_{\mathbf{x}_k}} = \mathbf{H}_k(\hat{\boldsymbol{\theta}}) \; ; \; \hat{\mathbf{F}}_{k-1} = \left.\frac{\partial \mathbf{f}_{k-1}(\boldsymbol{x}_{k-1}, \hat{\boldsymbol{\omega}})}{\partial \boldsymbol{x}^T_{k-1}}\right|_{\mathbf{m}_{\mathbf{x}_{k-1}}} = \mathbf{F}_{k-1}(\hat{\boldsymbol{\omega}}). \tag{31a}$$

Moreover, in this case,

$$\frac{\partial \mathbf{f}_{k-1}(\mathbf{x}_{k-1},\hat{\boldsymbol{\omega}})}{\partial \boldsymbol{\omega}^T}(\boldsymbol{\omega}-\hat{\boldsymbol{\omega}}) = \frac{\partial(\mathbf{F}_{k-1}(\hat{\boldsymbol{\omega}})\mathbf{x}_{k-1})}{\partial \boldsymbol{\omega}^T}(\boldsymbol{\omega}-\hat{\boldsymbol{\omega}}) = \frac{\partial}{\partial \boldsymbol{\omega}^T}\left(\sum_p \mathbf{f}_{k-1}^p(\hat{\boldsymbol{\omega}})(\mathbf{x}_{k-1})_p\right)(\boldsymbol{\omega}-\hat{\boldsymbol{\omega}})$$

$$= \sum_p \frac{\partial \mathbf{f}_{k-1}^p(\hat{\boldsymbol{\omega}})}{\partial \boldsymbol{\omega}^T}(\boldsymbol{\omega}-\hat{\boldsymbol{\omega}})(\mathbf{x}_{k-1})_p \simeq \sum_p (\mathbf{f}_{k-1}^p(\hat{\boldsymbol{\omega}}+(\boldsymbol{\omega}-\hat{\boldsymbol{\omega}})) - \mathbf{f}_{k-1}^p(\hat{\boldsymbol{\omega}}))(\mathbf{x}_{k-1})_p$$

$$\simeq \sum_p (\mathbf{f}_{k-1}^p(\boldsymbol{\omega}) - \mathbf{f}_{k-1}^p(\hat{\boldsymbol{\omega}}))(\mathbf{x}_{k-1})_p \simeq (\mathbf{F}_{k-1}(\boldsymbol{\omega}) - \mathbf{F}_{k-1}(\hat{\boldsymbol{\omega}}))\mathbf{x}_{k-1} = d\mathbf{F}_{k-1}\mathbf{x}_{k-1}, \tag{31b}$$

$$\frac{\partial \mathbf{h}_k(\mathbf{x}_k,\hat{\boldsymbol{\theta}})}{\partial \boldsymbol{\theta}^T}(\boldsymbol{\theta}-\hat{\boldsymbol{\theta}}) = \frac{\partial(\mathbf{H}_k(\hat{\boldsymbol{\theta}})\mathbf{x}_k)}{\partial \boldsymbol{\theta}^T}(\boldsymbol{\theta}-\hat{\boldsymbol{\theta}}) = \frac{\partial}{\partial \boldsymbol{\theta}^T}\left(\sum_p \mathbf{h}_k^p(\hat{\boldsymbol{\theta}})(\mathbf{x}_k)_p\right)(\boldsymbol{\theta}-\hat{\boldsymbol{\theta}})$$

$$= \sum_p \frac{\partial \mathbf{h}_k^p(\hat{\boldsymbol{\theta}})}{\partial \boldsymbol{\theta}^T}(\boldsymbol{\theta}-\hat{\boldsymbol{\theta}})(\mathbf{x}_k)_p \simeq \sum_p (\mathbf{h}_k^p(\hat{\boldsymbol{\theta}}+(\boldsymbol{\theta}-\hat{\boldsymbol{\theta}})) - \mathbf{h}_k^p(\hat{\boldsymbol{\theta}}))(\mathbf{x}_k)_p$$

$$\simeq \sum_p (\mathbf{h}_k^p(\boldsymbol{\theta}) - \mathbf{h}_k^p(\hat{\boldsymbol{\theta}}))(\mathbf{x}_k)_p \simeq (\mathbf{H}_k(\boldsymbol{\theta}) - \mathbf{H}_k(\hat{\boldsymbol{\theta}}))\mathbf{x}_k = d\mathbf{H}_k\mathbf{x}_k, \tag{31c}$$

and (29) reduces to (13b). It is noteworthy that the above identities shows that (27) and (29) coincide with (13a) to (13b) when the nonlinear SSM becomes linear, which confirms the relevance of (27) to (29) as a first-order approximation of (23a) and (23b).

3.6 | Mitigation of parametric modeling errors on the nonlinear state and measurement system functions

Note that if $\mathbb{E}[\hat{\mathbf{x}}_{k-1|k-1}^b] = \mathbf{m}_{\mathbf{x}_{k-1}}$, we can write that

$$\mathbb{E}[\hat{\mathbf{x}}_{k|k}(\mathbf{L}_k) - \mathbf{x}_k] \simeq \mathbb{E}[\boldsymbol{\varepsilon}_k(\mathbf{L}_k)] \simeq -(\mathbf{I}-\mathbf{L}_k\hat{\mathbf{H}}_k)\mathbb{E}\left[\frac{\partial \mathbf{f}_{k-1}(\mathbf{x}_{k-1},\hat{\boldsymbol{\omega}})}{\partial \boldsymbol{\omega}^T}\right](\boldsymbol{\omega}-\hat{\boldsymbol{\omega}}) + \mathbf{L}_k\mathbb{E}\left[\frac{\partial \mathbf{h}_k(\mathbf{x}_k,\hat{\boldsymbol{\theta}})}{\partial \boldsymbol{\theta}^T}\right](\boldsymbol{\theta}-\hat{\boldsymbol{\theta}}). \tag{32}$$

Then we can conclude that

$$\forall(\boldsymbol{\omega}-\hat{\boldsymbol{\omega}}), \forall(\boldsymbol{\theta}-\hat{\boldsymbol{\theta}}),\ \mathbb{E}[\boldsymbol{\varepsilon}_k(\mathbf{L}_k)] \simeq \mathbf{0} \ \Leftrightarrow\ \begin{cases} \mathbf{L}_k\mathbb{E}\left[\frac{\partial \mathbf{h}_k(\mathbf{x}_k,\hat{\boldsymbol{\theta}})}{\partial \boldsymbol{\theta}^T}\right] = \mathbf{0} \\ (\mathbf{I}-\mathbf{L}_k\hat{\mathbf{H}}_k)\mathbb{E}\left[\frac{\partial \mathbf{f}_{k-1}(\mathbf{x}_{k-1},\hat{\boldsymbol{\omega}})}{\partial \boldsymbol{\omega}^T}\right] = \mathbf{0} \end{cases}, \tag{33}$$

which defines a sensible set of constraints in order to mitigate the bias introduced by parametric modeling errors in the nonlinear system functions, by means of a LCEKF. However, in most cases, the expectations are probably not computable, and will be approximated by

$$d\mathbf{F}_{k-1} = \mathbb{E}\left[\frac{\partial \mathbf{f}_{k-1}(\mathbf{x}_{k-1},\hat{\boldsymbol{\omega}})}{\partial \boldsymbol{\omega}^T}\right] \simeq \frac{\partial \mathbf{f}_{k-1}\left(\hat{\mathbf{x}}_{k-1|k-1}^b,\hat{\boldsymbol{\omega}}\right)}{\partial \boldsymbol{\omega}^T}\ ;\ d\mathbf{H}_k = \mathbb{E}\left[\frac{\partial \mathbf{h}_k(\mathbf{x}_k,\hat{\boldsymbol{\theta}})}{\partial \boldsymbol{\theta}^T}\right] \simeq \frac{\partial \mathbf{h}_k(\hat{\mathbf{x}}_{k|k-1}^b,\hat{\boldsymbol{\theta}})}{\partial \boldsymbol{\theta}^T},$$

leading to the following implementable LCs

$$\begin{cases} \mathbf{L}_k\frac{\partial \mathbf{h}_k(\hat{\mathbf{x}}_{k|k-1}^b,\hat{\boldsymbol{\theta}})}{\partial \boldsymbol{\theta}^T} = \mathbf{0} \\ (\mathbf{I}-\mathbf{L}_k\hat{\mathbf{H}}_k)\frac{\partial \mathbf{f}_{k-1}(\hat{\mathbf{x}}_{k-1|k-1}^b,\hat{\boldsymbol{\omega}})}{\partial \boldsymbol{\omega}^T} = \mathbf{0} \end{cases}. \tag{34}$$

As it has been shown in Reference 21, if $\text{rank}(d\mathbb{F}_{k-1}) = P_k$, then the introduction of constraints (34) cancels the main merit of the KF, that is, the incorporation of the previous observations in the state estimation process. Thus, it is worth using the LCEKF only if $\text{rank}(d\mathbb{F}_{k-1}) = R_k < P_k$, and then follow the approach in (14a) to (14c) for the constraint on $d\mathbb{F}_{k-1}$.

As in the standard EKF, computable forms of $\hat{\mathbf{F}}_{k-1}$ and $\hat{\mathbf{H}}_k$ are: $\hat{\mathbf{F}}_{k-1} = \left.\frac{\partial \mathbf{f}_{k-1}(\boldsymbol{x}_{k-1},\hat{\boldsymbol{\omega}})}{\partial \boldsymbol{x}_{k-1}^T}\right|_{\hat{\mathbf{x}}^b_{k-1|k-1}}$ and $\hat{\mathbf{H}}_k = \left.\frac{\partial \mathbf{h}_k(\boldsymbol{x}_k,\hat{\boldsymbol{\theta}})}{\partial \boldsymbol{x}_k^T}\right|_{\hat{\mathbf{x}}^b_{k|k-1}}$.

In terms of computational complexity, as for the KF vs LCKF case, the same applies for the comparison between the EKF and the LCEKF, which are the first-order approximations of the KF and LCKF solutions, respectively. That is, the EKF gain is computed as for the KF but with the corresponding linearized $\mathbf{F}_{k-1}$ and $\mathbf{H}_k$. For the LCEKF, we have to apply the corresponding constraints, which lead to a gain computation similar to the one in the LCKF but with the linearized system model. Therefore, again, the LCEKF can be used in any real-life application where the EKF is the gold standard solution with a marginal additional computational cost.

3.7 | Robust LCEKF under mismatched inputs

So far we have discussed the impact (Section 3.2) and mitigation (Section 3.6) of parametric modeling errors in both process and measurement nonlinear functions via LCs (ie, $\boldsymbol{\omega} \neq \hat{\boldsymbol{\omega}}$ and $\boldsymbol{\theta} \neq \hat{\boldsymbol{\theta}}$). But the proposed LCEKF framework is in fact more powerful and can be used to mitigate other types of errors in the nonlinear dynamic system. For instance, an important problem in automatic control is the use of possibly mismatched (uncertain to a certain extent) command inputs, $\mathbf{u}_k$. This can be formulated in both linear and nonlinear SSM as a mismatched-true SSM pair similar to (5a) and (5b) or (21a) and (21b). Notice that inputs are typically considered within the process equation, thus in the following we do not rewrite the measurement equation which remains the same as above. We may consider two cases of interest, where the mismatched input is $\hat{\mathbf{u}}_{k-1} = \mathbf{u}_{k-1} + d\hat{\mathbf{u}}_{k-1}$:

- Case (1) Inputs in the nonlinear process equation:

$$\begin{aligned} \text{Mismatched} &: \mathbf{x}'_k = \mathbf{f}_{k-1}(\mathbf{x}'_{k-1}, \hat{\mathbf{u}}_{k-1}) + \mathbf{w}_{k-1}, \\ \text{True} &: \mathbf{x}_k = \mathbf{f}_{k-1}(\mathbf{x}_{k-1}, \mathbf{u}_{k-1}) + \mathbf{w}_{k-1}. \end{aligned} \tag{35a}$$

  Following the analysis in Sections 3.2 to 3.6 we can define the set of constraints (and the corresponding approximation) to be used within the LCEKF in order to mitigate the error induced by mismatched inputs, as

$$\forall d\hat{\mathbf{u}}_{k-1},\ \mathbb{E}[\boldsymbol{\varepsilon}_k(\mathbf{L}_k)] \simeq \mathbf{0} \ \Leftrightarrow\ (\mathbf{I} - \mathbf{L}_k\hat{\mathbf{H}}_k)\mathbb{E}\left[\frac{\partial \mathbf{f}_{k-1}(\mathbf{x}_{k-1}, \hat{\mathbf{u}}_{k-1})}{\partial \mathbf{u}_{k-1}^T}\right] \simeq (\mathbf{I} - \mathbf{L}_k\hat{\mathbf{H}}_k)\underbrace{\frac{\partial \mathbf{f}_{k-1}(\hat{\mathbf{x}}^b_{k-1|k-1}, \hat{\mathbf{u}}_{k-1})}{\partial \mathbf{u}_{k-1}^T}}_{d\mathbb{F}_{k-1}} = \mathbf{0}, \tag{35b}$$

  which are worth to be used only in the case that $\text{rank}(d\mathbb{F}_{k-1}) = R_k < P_k$, and thus we follow the approach in (14a) to (14c) for the constraint on $d\mathbb{F}_{k-1}$.[21]
- Case (2) Additive command input:

$$\begin{aligned} \text{Mismatched} &: \mathbf{x}'_k = \mathbf{f}_{k-1}(\mathbf{x}'_{k-1}) + \mathbf{g}_{k-1}(\hat{\mathbf{u}}_{k-1}) + \mathbf{w}_{k-1}, \\ \text{True} &: \mathbf{x}_k = \mathbf{f}_{k-1}(\mathbf{x}_{k-1}) + \mathbf{g}_{k-1}(\mathbf{u}_{k-1}) + \mathbf{w}_{k-1}. \end{aligned} \tag{36a}$$

  In this case, we can further elaborate the set of constraints to mitigate the nonlinear input mismatch in (35b), where

$$d\mathbf{F}_{k-1} = \left.\frac{\partial(\mathbf{f}_{k-1}(\mathbf{x}_{k-1}) + \mathbf{g}_{k-1}(\mathbf{u}_{k-1}))}{\partial \mathbf{u}_{k-1}^T}\right|_{(\hat{\mathbf{x}}^b_{k-1|k-1}, \hat{\mathbf{u}}_{k-1})} = \frac{\partial \mathbf{g}_{k-1}(\hat{\mathbf{u}}_{k-1})}{\partial \mathbf{u}_{k-1}^T} = d\mathbb{G}_{k-1}, \tag{36b}$$

  and then the set of constraints becomes simply

$$\mathbf{L}_k\hat{\mathbf{H}}_k d\mathbb{G}_{k-1} = d\mathbb{G}_{k-1}, \tag{36c}$$

  which are worth to be used only in the case that $\text{rank}(d\mathbb{G}_{k-1}) = R_k < P_k$, and thus we follow the approach in (14a) to (14c) for the constraint on $d\mathbb{G}_{k-1}$.[21]

4 | VEHICLE NAVIGATION DYNAMIC MODEL

4.1 | Three-wheeled vehicle nonlinear state model

The so-called three-wheeled vehicle dynamic model, that is, the Ackerman model, can be used to model the kinematic behavior of most part of vehicles with three and four wheels. As it is shown in Figure 1, it consists of two main wheels which provide the vehicle speed, and a third wheel which controls the vehicle direction. The configuration can be described without ambiguity by a five-dimensional state vector $\mathbf{x}_k$ composed of the vehicle coordinates, angular deviations with respect to the vehicle path, linear velocity and the steering angle denoted, respectively, x, y, θ, V, and ψ, that is,

$$\mathbf{x}_k = (x_k, y_k, \theta_k, V_k, \psi_k)^T. \tag{37}$$

From Figure 1, the turn radius ρ is given by

$$\rho = \frac{D}{\tan(\psi)}, \tag{38a}$$

where D denotes the distance from the front wheel to the rear axle. From Figure 2, the following differential kinematics equations can be formulated

$$\begin{cases} \Delta x = x' - x = S\ \cos(\theta + \frac{\Delta\theta}{2}) \\ \Delta y = y' - y = S\ \sin(\theta + \frac{\Delta\theta}{2}) \\ \Delta\theta = \theta' - \theta = L/\rho \end{cases} \quad \begin{cases} L = V\Delta t \\ \Delta\theta = L/\rho = \frac{V\Delta t\ \tan(\psi)}{D} \\ S = 2\rho\ \sin\left(\frac{\Delta\theta}{2}\right) = \frac{2V\Delta t\ \tan(\psi)}{D}\ \sin\left(\frac{V\Delta t\ \tan(\psi)}{2\ D}\right) = V\Delta t\ \mathrm{sinc}\left(\frac{V\Delta t\ \tan(\psi)}{2\ D}\right) \end{cases}$$

leading to

$$\begin{cases} \Delta x = V\Delta t\ \mathrm{sinc}\left(\frac{V\Delta t\ \tan(\psi)}{2\ D}\right)\cos\left(\theta + \frac{V\Delta t\ \tan(\psi)}{2\ D}\right) \\ \Delta y = V\Delta t\ \mathrm{sinc}\left(\frac{V\Delta t\ \tan(\psi)}{2\ D}\right)\sin\left(\theta + \frac{V\Delta t\ \tan(\psi)}{2\ D}\right) \\ \Delta\theta = \frac{V\Delta t\ \tan(\psi)}{D} \end{cases}$$

Thus, a discrete nonlinear state model for the three-wheeled vehicle model is

$$\mathbf{x}_k = \mathbf{f}(\mathbf{x}_{k-1}, D) + \mathbf{u}_{k-1} + \mathbf{w}_{k-1},\ \mathbf{f}(\mathbf{x}, D) = \begin{pmatrix} x \\ y \\ \theta \\ V \\ \psi \end{pmatrix} + \begin{pmatrix} V\Delta t\ sinc\left(\frac{V\Delta t\ \tan(\psi)}{2\ D}\right)cos\left(\theta + \frac{V\Delta t\ \tan(\psi)}{2\ D}\right) \\ V\Delta t\ \mathrm{sinc}\left(\frac{V\Delta t\ \tan(\psi)}{2\ D}\right)\sin\left(\theta + \frac{V\Delta t\ \tan(\psi)}{2\ D}\right) \\ \frac{V\Delta t\ \tan(\psi)}{D} \\ 0 \\ 0 \end{pmatrix}, \tag{39a}$$

$\mathbf{u}_{k-1}^T = (0, 0, 0, \Delta V_{k-1}, \Delta\psi_{k-1})$ is the motion input command, and $\mathbf{w}_{k-1}$ is a state noise modeling the fact that there is a possible discrepancy between the desired motion command and the one actually taken into account,

$$\mathbf{w}_{k-1} \sim \mathcal{N}(0, \mathbf{C}_\mathbf{w}), \mathbf{C}_\mathbf{w} = \begin{bmatrix} \mathbf{0} & \mathbf{0} \\ \mathbf{0} & \begin{bmatrix} \sigma_V^2 & 0 \\ 0 & \sigma_\psi^2 \end{bmatrix} \end{bmatrix} \tag{39b}$$

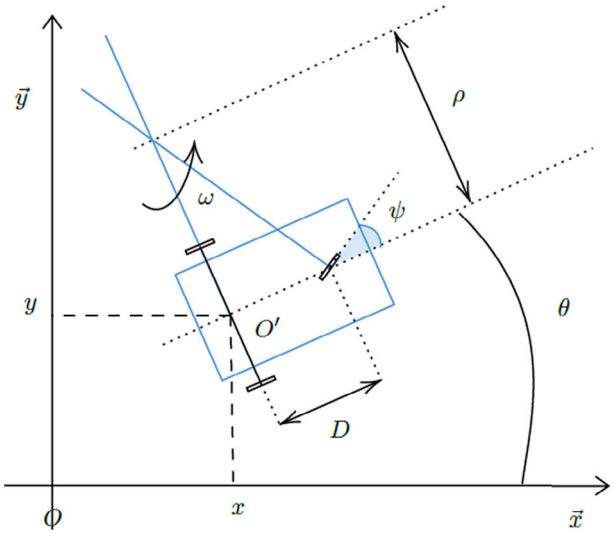

FIGURE 1 Three-wheeled vehicle model [Colour figure can be viewed at wileyonlinelibrary.com]

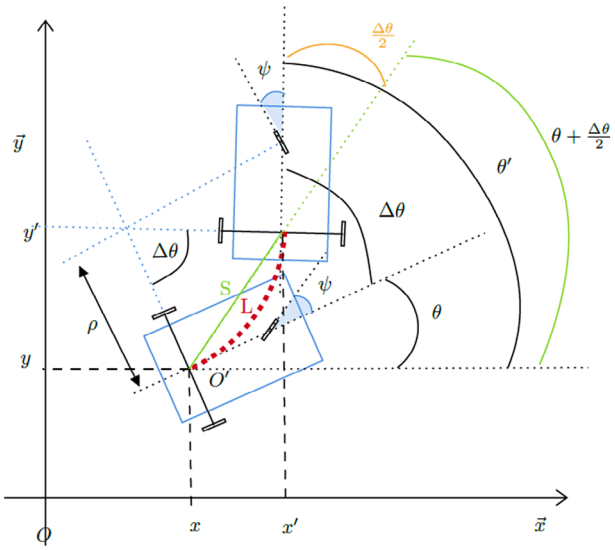

FIGURE 2 Three-wheeled vehicle model in movement [Colour figure can be viewed at wileyonlinelibrary.com]

4.2 | Nonlinear measurement model

A known technique for precisely locating an autonomous vehicle is to equip the vehicle with an optical or infrared scanner that is capable of measuring the position of a beacon. The measurement principle is shown in Figure 3, where the vehicle is located in a global coordinate frame (xOy) at position $O' = (x, y)$. The sensor installed in the vehicle measures the beacon position B with respect to the vehicle (body) coordinate frame (x'O'y'), that is

$$\begin{pmatrix} x'_B \\ y'_B \end{pmatrix} = \mathbf{R}(-\theta) \begin{pmatrix} x_B - x \\ y_B - y \end{pmatrix} + \mathbf{n}_k, \ \mathbf{R}(\theta) = \begin{bmatrix} cos(\theta) & -sin(\theta) \\ sin(\theta) & cos(\theta) \end{bmatrix}, \tag{40a}$$

where $\mathbf{n}_k$ denotes the additive Gaussian measurement noise,

$$\mathbf{n}_k \sim \mathcal{N}(\mathbf{0}, \mathbf{C}_n), \quad \mathbf{C}_n = \begin{bmatrix} \sigma^2_{x'} & 0 \\ 0 & \sigma^2_{y'} \end{bmatrix}. \tag{40b}$$

The nonlinear measurement vector $\mathbf{y}_k$ then reads

FIGURE 3 Vehicle coordinate system [Colour figure can be viewed at wileyonlinelibrary.com]

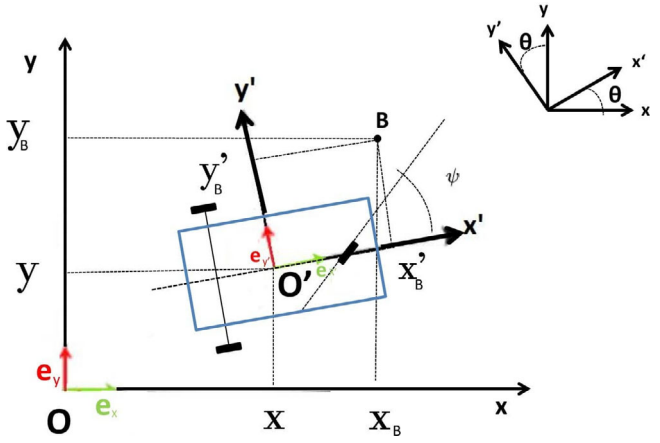

$$\mathbf{y}_k = \begin{pmatrix} (x'_B)_k \\ (y'_B)_k \\ \theta_k \\ V_k \\ \psi_k \end{pmatrix} = \begin{bmatrix} \mathbf{R}(-\theta_k) & \mathbf{0} \\ \mathbf{0} & \mathbf{I}_3 \end{bmatrix} \begin{pmatrix} x_B - x_k \\ y_B - y_k \\ \theta_k \\ V_k \\ \psi_k \end{pmatrix} + \mathbf{v}_k = \mathbf{h}(\mathbf{x}_k) + \mathbf{v}_k,\ \mathbf{h}(\mathbf{x}) = \begin{pmatrix} cos(\theta)(x_B - x) + sin(\theta)(y_B - y) \\ -sin(\theta)(x_B - x) + cos(\theta)(y_B - y) \\ \theta \\ V \\ \psi \end{pmatrix}. \quad (41a)$$

The angular deviation with respect to the vehicle path θ and the velocity V are navigation information provided, respectively, by an inertial navigation system (INS) and an odometer. ψ_{m} is the steering information obtained from a steering angle sensor. The additive measurement noise $\mathbf{v}_k$ is modeled as white Gaussian noise, that is,

$$\mathbf{v}_k \sim \mathcal{N}(\mathbf{0}, \mathbf{C}_{\mathbf{v}}),\ \mathbf{C}_{\mathbf{v}} = \begin{bmatrix} \mathbf{C_n} & \mathbf{0} \\ \mathbf{0} & \begin{bmatrix} \sigma^2_{\theta_{\mathrm{INS}}} & 0 & 0 \\ 0 & \sigma^2_{V_{\mathrm{Odo}}} & 0 \\ 0 & 0 & \sigma^2_{\psi_{\mathrm{m}}} \end{bmatrix} \end{bmatrix}, \quad (41b)$$

where $\sigma^2_{\theta_{\mathrm{INS}}}$, $\sigma^2_{\psi_{\mathrm{Odo}}}$ are the variances of INS-based and odometer-based observables, and $\sigma^2_{\psi_{\mathrm{m}}}$ depends on the quality of the steering angle sensor.

5 | ROBUST VEHICLE NAVIGATION ILLUSTRATIVE RESULTS

5.1 | Mismatched nonlinear state and measurement models

We consider the case where we may have an imperfect knowledge on the parametric state and observation model, (39a) and (41a). Indeed, in practice, due to initial calibration errors, aging or thermal expansion, the distance D may not be perfectly known and/or the scanner coordinate frame may not be perfectly aligned with the vehicle coordinate frame, leading to a deviation θ_d with respect to the vehicle path θ. In the latter case, the observation model (41a) becomes

$$\mathbf{h}(\mathbf{x}) \triangleq \mathbf{h}(\mathbf{x}, \theta_d) = \begin{pmatrix} \cos(\theta + \theta_d)(x_B - x) + \sin(\theta + \theta_d)(y_B - y) \\ -\sin(\theta + \theta_d)(x_B - x) + \cos(\theta + \theta_d)(y_B - y) \\ \theta \\ V \\ \psi \end{pmatrix}.$$

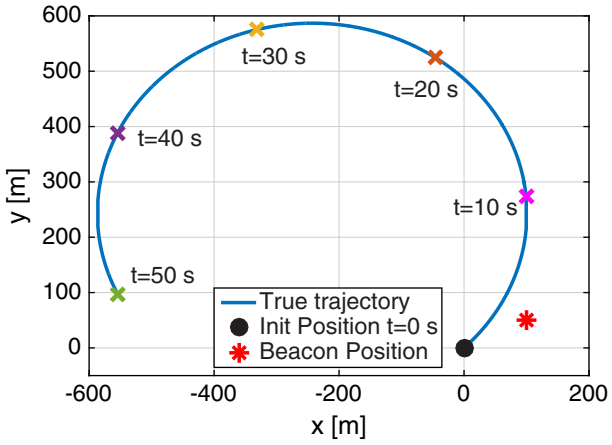

FIGURE 4 The two-dimensional trajectory of the vehicle [Colour figure can be viewed at wileyonlinelibrary.com]

Then, the implementation of the standard EKF computed with

$$\hat{\mathbf{F}}_k = \left.\frac{\partial \mathbf{f}(\mathbf{x}, \hat{D})}{\partial \mathbf{x}^T}\right|_{\hat{\mathbf{x}}^b_{k-1|k-1}}, \quad \hat{\mathbf{H}}_k = \left.\frac{\partial \mathbf{h}(\mathbf{x}, 0)}{\partial \mathbf{x}^T}\right|_{\hat{\mathbf{x}}^b_{k|k-1}}$$

may lead to a performance breakdown in case of an inaccurate assumed value of D, denoted $\hat{D}$, and/or the presence of $\theta_d \neq 0$. In order to improve the estimation accuracy we consider the use of a LCEKF incorporating the constraints in (34), which in this case are

$$(\mathbf{I} - \mathbf{L}_k \hat{\mathbf{H}}_k) d\mathbf{f}_{k-1} = \mathbf{0}, \; d\mathbf{f}_{k-1} = \left.\frac{\partial \mathbf{f}(\mathbf{x}, \hat{D})}{\partial D}\right|_{\hat{\mathbf{x}}^b_{k-1|k-1}} \tag{42a}$$

$$\mathbf{L}_k d\mathbf{h}_k = \mathbf{0}, \; d\mathbf{h}_k = \left.\frac{\partial \mathbf{h}(\mathbf{x}, 0)}{\partial \theta_d}\right|_{\hat{\mathbf{x}}^b_{k|k-1}} \tag{42b}$$

and lead to $\mathbf{\Delta}_k = \begin{bmatrix} \hat{\mathbf{H}}_k d\mathbf{f}_{k-1} & d\mathbf{h}_k \end{bmatrix}$ and $\mathbf{T}_k = \begin{bmatrix} d\mathbf{f}_{k-1} & \mathbf{0} \end{bmatrix}$.

5.2 | Illustrative results

As an example, we consider the following setup: $\mathbf{x}_0 = (0, 0, 45°, 30, 1°)^T$, $\mathbf{C}_{\mathbf{x}_0} = \mathbf{0}$, $\mathbf{u}_{k-1} = \mathbf{0}$, $\Delta t = 1$ ms, $\sigma_V = 1$ m.s^{-1}, $\sigma_\psi = \sqrt{0.1}$ °, for the state model (39a), and, $B = (100, 50)$, $\sigma_{x'} = 1$ m, $\sigma_{y'} = 1$ m, $\sigma_{\theta_{\text{INS}}} = \sqrt{0.1}$ °, $\sigma_{V_{\text{Odo}}} = 1$ m.s^{-1}, $\sigma_{\psi_{\text{m}}} = \sqrt{0.1}$ °, for the measurement model (41a). D_v denotes the true value of D ($D_v = 3$ m), $\Delta D = D_v - \hat{D}$ denotes the deviation between D_v and the assumed distance $\hat{D}$. The true two-dimensional (2D) vehicle trajectory, that is,

$$\mathbf{x}_k = \mathbf{f}(\mathbf{x}_{k-1}, D_v) + \mathbf{w}_{k-1}, \tag{43}$$

is displayed in Figure 4. Its quasi-circular shape, not centered on the beacon location B, has been designed to test the robustness of various LCEKFs against a large range of θ and (x'_B, y'_B).

We compare the following filters:

- The (mismatched) standard EKF which does not incorporate constraints into the Kalman process,
- The so-called LCEKF-D is a LCEKF which incorporates only the state constraint (42a),
- The so-called LCEKF-θ is a LCEKF which incorporates only the measurement constraint (42b),
- The so-called LCEKF-θ-D is a LCEKF which incorporates both constraints (42a) and (42b).

FIGURE 5 MSE w.r.t. time, $\Delta D = 0$ and $\theta_d = 0°$. MSE, mean square error [Colour figure can be viewed at wileyonlinelibrary.com]

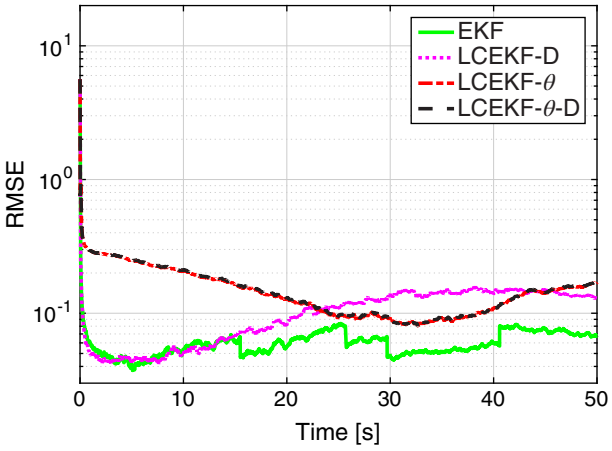

FIGURE 6 MSE w.r.t. time, $\Delta D = 0$ and $\theta_d = 0.1°$. MSE, mean square error [Colour figure can be viewed at wileyonlinelibrary.com]

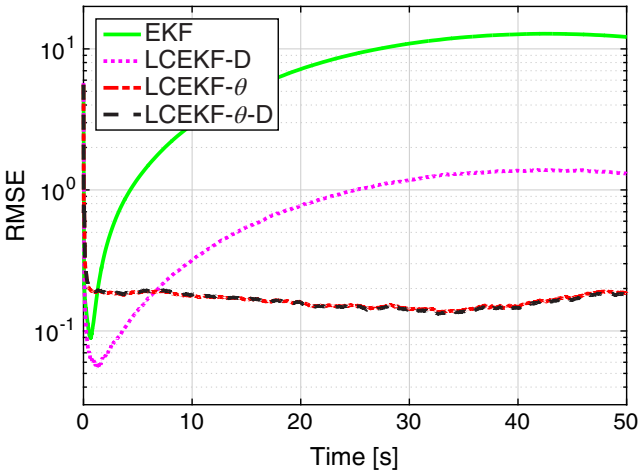

The measure of performance is the total root MSE (RMSE) of the estimated states (from 500 Monte Carlo runs), given by

$$\text{RMSE} = \sqrt{\mathbb{E}\{(\mathbf{x}_k - \hat{\mathbf{x}}_{k|k})^T(\mathbf{x}_k - \hat{\mathbf{x}}_{k|k})\}}. \tag{44}$$

The results are summarized in Figures 5 to 8, which show the MSE w.r.t. time t,

- Figure 5: MSE w.r.t. t where $\Delta D = 0$ and $\theta_d = 0°$,
- Figure 6: MSE w.r.t. t where $\Delta D = 0$ and $\theta_d = 0.1°$,
- Figure 7: MSE w.r.t. t where $\Delta D = 0.7$ m and $\theta_d = 0°$,
- Figure 8: MSE w.r.t. t where $\Delta D = 0.7$ m and $\theta_d = 0.1°$.

These results allow to draw the following conclusions:

(i) If the parametric model is perfectly known (Figure 5), that is, we have no mismatch and therefore $\Delta D = 0$ and $\theta_d = 0°$, as expected the EKF exhibits a good performance since it matches the true SSM. Interestingly, the LCEKF-D, LCEKF-θ, and LCEKF-θ-D exhibit a performance close to the EKF, but with a MSE degradation induced by the use of constraints which consume additional degrees of freedom.

(ii) If the parametric model is not perfectly known (Figures 6-8), that is, there exists a model mismatch on D and/or θ, the proposed LCEKFs (LCEKF-D, LCEKF-θ, and LCEKF-θ-D) show better performance in comparison with the mismatched EKF, since the proposed filters exploit LCs to mitigate the effect of an erroneous knowledge about the

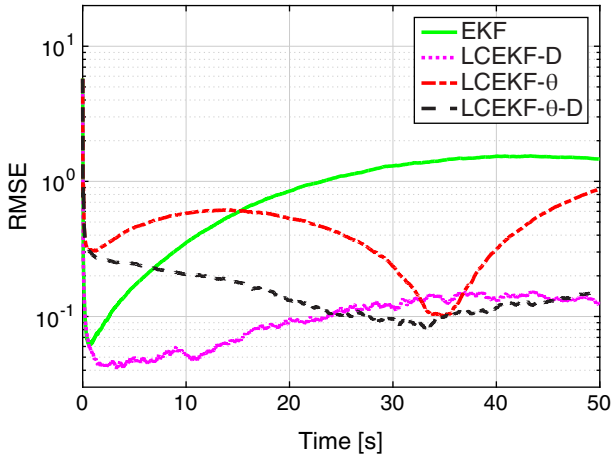

FIGURE 7 MSE w.r.t. time, $\Delta D = 0.7$ m and $\theta_d = 0°$. MSE, mean square error [Colour figure can be viewed at wileyonlinelibrary.com]

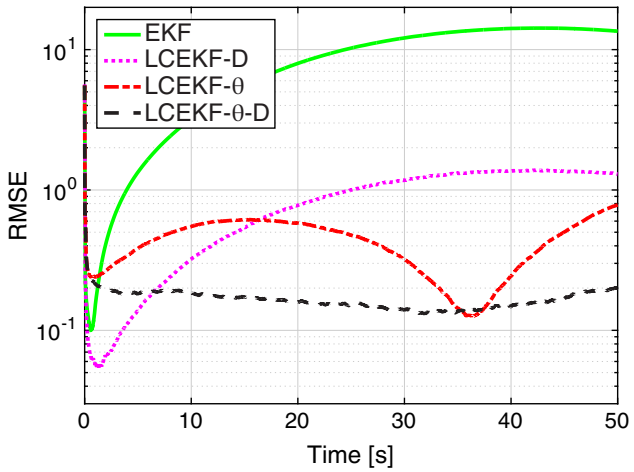

FIGURE 8 MSE w.r.t. time, $\Delta D = 0.7$ m and $\theta_d = 0.1°$. MSE, mean square error [Colour figure can be viewed at wileyonlinelibrary.com]

dynamic model. The performance difference among LCEKFs mainly depends on the type of mismatch and the LCs included within the filter formulation.

(iii) The proposed LCEKF-θ-D which takes both mismatches into account is robust to reasonable deviations, that is, $\theta_d = 0.1°$ (Figure 6), $\Delta D = 0.7$ m (Figure 7) or both $\Delta D = 0.7$ m and $\theta_d = 0.1°$ (Figure 8), whereas the EKF exhibits a performance breakdown as modeling errors increase, that is, state, measurement or in both equations.

(iv) Both the LCEKF-D (only considering the state mismatch ΔD) and LCEKF-θ (only considering the measurement mismatch θ_d) have inherent limitations as illustrated, respectively, in Figures 6 and 7. Since the LCEKF-D does not mitigate the measurement model matrices mismatch its performance is shown to rapidly degrade in Figure 6, but with an asymptotic performance which is lower than for the standard (mismatched) EKF. The latter implies that the state constraint has an impact on the measurement error propagation. Similarly, the LCEKF-θ does not incorporate the state constraint in the filtering process, and therefore it exhibits a poor performance under state model mismatch, as shown in Figure 7. Again, in this case the LCEKF-θ performance is better than the EKF, then the measurement constraint has an impact on the state error propagation.

(v) To summarize, notice that a minimal model mismatch, such as $\theta_d = 0.1°$, completely spoils the standard EKF solution. Therefore, taking into account possible model mismatches is fundamental in real-life applications, which clearly shows the need for robust solutions. The new LCEKF has been shown to be a promising solution to cope with such modeling errors and a powerful robust filtering approach. Considering all possible mismatches, that is, LCEKF-θ-D in our case study, provides a robust solution under model mismatch. Indeed, notice that in any case, the RMSE for the 2D position obtained with the LCEKF-θ-D is always below 20 cm. By contrast, the corresponding RMSE obtained with the mismatched EKF is at least one order of magnitude greater.

6 | CONCLUSION AND OUTLOOK

Even if a lot of contributions derived robust filtering approaches to counteract uncertain noise statistics and/or outliers in the system model, very few works explored the problem of model mismatch in the system process and measurement functions. In this contribution we explored the use of LCs in order to robustify standard nonlinear filtering techniques. First, we investigated how to incorporate LCs within the EKF and derived a new LCEKF. Then, we discussed how this new LCEKF can be used to mitigate both parametric modeling errors in the nonlinear process and measurement functions. In addition, it was shown by considering the problem of system models with mismatched inputs that the proposed framework is rather general. A robust vehicle navigation problem was used to show (i) the impact of mismatches on standard filtering techniques, (ii) that using LCs may be an efficient way to cope with both process and measurement model mismatches, (iii) and that the use of a LCEKF provides a tremendous performance improvement w.r.t. the mismatched filter, but the price to be paid is a performance degradation w.r.t. the optimal under nominal conditions.

These results show a promising new framework, which certainly deserves to be further analyzed and extended to more general settings. In that perspective one could think on the use of constraints within the sigma-point Gaussian filtering framework, that is, Unscented KF, Cubature KF, Quadrature KF,[39] or more general sequential Monte Carlo solutions to cope with non-Gaussianity, but notice that this is a nontrivial extension because the constrained propagation of such deterministic or random samples through a nonlinear function and the correct approximation of the final Bayesian filtering integrals has never been addressed, thus it will require a dedicated and thorough analysis.

ACKNOWLEDGEMENTS

This work has been partially supported by the DGA/AID projects 2018.60.0072.00.470.75.01 and 2019.65.0068.00.470.75.01, and the Agence Nationale de la Recherche project ANR-17-CE22-0001-01.

CONFLICT OF INTEREST

The authors declare no potential conflict of interests.

ORCID

Jordi Vilà-Valls https://orcid.org/0000-0001-7858-4171

REFERENCES

1. Crassidis JL, Junkins JL. *Optimal Estimation of Dynamic Systems*. 2nd ed. Boca Raton, FL: CRC Press, Taylor & Francis Group; 2012.
2. Diniz PSR. *Adaptive Filtering: Algorithms and Practical Implementation*. 4th ed. Switzerland: Springer; 2013.
3. Simon D. *Optimal State Estimation: Kalman, H-Infinity, and Nonlinear Approaches*. Hoboken, NJ: John Wiley & Sons; 2013.
4. Groves PD. *Principles of GNSS, Inertial, and Multisensor Integrated Navigation Systems*. 2nd ed. Norwood, MA: Artech House; 2013.
5. Anderson B, Moore JB. *Optimal Filtering*. Englewood Cliffs, NJ: Prentice-Hall; 1979.
6. Ito K, Xiong K. Gaussian filters for nonlinear filtering problems. *IEEE Trans Automat Control*. 2000;45(5):910-927.
7. Arasaratnam I, Haykin S. Cubature Kalman filters. *IEEE Trans Automat Control*. 2009;54(6):1254-1269.
8. Djurić P, Kotecha JH, Zhang J, et al. Particle filtering. *IEEE Signal Process Mag*. 2003;140(2):19-38.
9. Dunik J, Straka O, Kost O, Havlik J. Noise covariance matrices in state-space models: a survey and comparison of estimation methods - Part I. *Int J Adapt Control Signal Process*. 2017;31:1505-1543.
10. Ardeshiri T, Ozkan E, Orguner U, Gustafsson F. Approximate Bayesian smoothing with unknown process and measurement noise covariances. *IEEE Signal Process Lett*. 2015;22(12):2450-2454.
11. Agamennoni G, Nieto JI, Nebot EM. Approximate inference in state-space models with heavy-tailed noise. *IEEE Trans Sig Process*. 2012;60(10):5024-5037.
12. Nurminen H, Ardeshiri T, Piché R, Gustafsson F. Robust inference for state-space models with skewed measurement noise. *IEEE Signal Process Lett*. 2015;22(11):1898-1902.
13. Huang Y, Zhang Y, Shi P, Wu Z, Qian J, Chambers J. Robust Kalman filters based on gaussian scale mixture distribution with application to target tracking. *IEEE Trans Syst Man Cybern*. 2019;49(10):2082-2096.
14. Vilà-Valls J, Closas P. NLOS mitigation in indoor localization by Marginalized Monte Carlo Gaussian smoothing. *EURASIP J Adv Sig Process*. 2017;62 (2017).
15. Zoubir AM, Koivunen V, Ollila E, Muma M. *Robust Statistics for Signal Processing*. Cambridge, UK: Cambridge University Press; 2018.
16. Gandhi MA, Mili L. Robust Kalman filter based on a generalized maximum-likelihood-type estimator. *IEEE Trans Signal Process*. 2010;58(5):2509-2520.
17. Chang L, Li K. Unified form for the robust Gaussian information filtering based on M-estimate. *IEEE Signal Process Lett*. 2017;24(4):412-416.

18. Chaumette E. Minimum variance distortionless response estimators for linear discrete state-space models. *IEEE Trans Autom Control*. 2017;62(4):2048-2055.
19. Chaumette E. On LMVDR estimators for LDSS models: conditions for existence and further applications. *IEEE Trans Autom Control*. 2019;64(6):2598-2605.
20. Li XR, Jilkov VP. Survey of maneuvering target tracking. Part V: multiple-model methods. *IEEE Trans Aerosp Elec Syst*. 2005;41(4):1255-1321.
21. Vilà-Valls J, Vivet D, Chaumette E, Vincent F, Closas P. Recursive linearly constrained wiener filter for robust multi-channel signal processing. *Signal Processing*. 2020;167:107291.
22. Chaumette E, Vincent F, Vilà-Valls J. Linearly constrained Wiener filter estimates for linear discrete state-space models. Paper presented at: Proceedings of the Asilomar Conference on Signals, Systems, and Computers. Pacific Grove, CA; 2018.
23. Teixeira BOS. Gain-constrained Kalman filtering for linear and nonlinear systems. *IEEE Trans Signal Process*. 2008;56(9):4113-4123.
24. Jazwinski AH. *Stochastic Processes and Filtering Theory*. Mineola, NY: Dover Publications Inc; 2007.
25. Spall JC, Wall KD. Asymptotic distribution theory for the Kalman filter state estimator. *Commun Stat Theory Methods*. 1984;13(16):1981-2003.
26. Liu X. Stochastic stability condition for the extended Kalman filter with intermittent observations. *IEEE Trans Circ Syst II Exp Briefs*. 2016;64(3):334-338.
27. Li J, Stoica P. *Robust Adaptive Beamforming*. New York, NY: Wiley Online Library; 2006.
28. Vorobyov SA. Principles of minimum variance robust adaptive beamforming design. *Signal Process*. 2013;93(12):3264-3277.
29. Amor N, Rasool G, Bouaynaya NC. Constrained State Estimation a Review; 2018. arXiv preprint arXiv:1807.03463.
30. Sridhar U, Eric D, Keyu L. Constrained extended Kalman filter for nonlinear state estimation. *IFAC Proc Vols*. 2007;40:63-68.
31. Spong MW. *Robot Modeling and Control*. Vol 3. New York, NY: Wiley; 2006.
32. Simon D, Chia TL. Kalman filtering with state equality constraints. *IEEE Trans Aerosp Electron Syst*. 2002;38(1):128-136.
33. Wang LS, Chiang YT, Chang FR. Filtering method for nonlinear systems with constraints. *IEE Proc Control Theory Appl*. 2002;149(6):525-531.
34. Heffes H. The effect of erroneous models on the Kalman Filter response. *IEEE Trans Autom Control*. 1966;11(13):541-543.
35. Theodor Y, Shaked U. Robust discrete-time minimum-variance filtering. *IEEE Trans Signal Process*. 1996;44(2):181-189.
36. Trees HLV. *Optimum Array Processing*. New York, NY: Wiley-Interscience; 2002.
37. Vilà-Valls J, Chaumette E, Vincent F, Closas P. Modelling mismatch and noise statistics uncertainty in linear MMSE Estimation. Proceedings of the European Signal Processing Conference; 2019.
38. Horn RA, Johnson CR. *Matrix Analysis*. 2nd ed. Cambridge, UK: Cambridge University Press; 2013.
39. Roth M, Hendeby G, Gustafsson F. Nonlinear Kalman filters explained: a tutorial on moment computations and sigma point methods. *J Adv Inf Fusion*. 2016;11(1):47-70.

How to cite this article: Hrustic E, Ben Abdallah R, Vilà-Valls J, Vivet D, Pagès G, Chaumette E. Robust linearly constrained extended Kalman filter for mismatched nonlinear systems. *Int J Robust Nonlinear Control*. 2020;1–19. https://doi.org/10.1002/rnc.5305

APPENDIX A. EXPLICIT EXPRESSIONS FOR THE EKF APPROXIMATIONS

In the sequel we provide the explicit expression of $\frac{\partial \mathbf{f}_{k-1}(\mathbf{x}_{k-1})}{\partial \mathbf{x}_{k-1}^T}$ and $\frac{\partial \mathbf{f}_{k-1}(\mathbf{x}_{k-1})}{\partial D}$, where $\mathbf{f}_{k-1}(\mathbf{x}_{k-1}) = \mathbf{f}(\mathbf{x}_{k-1}, D)$, and $\mathbf{f}(\mathbf{x}, D) = (f_1(\mathbf{x}, D), f_2(\mathbf{x}, D), \ldots, f_5(\mathbf{x}, D))^T$ (39a):

$$\frac{\partial \mathbf{f}(\mathbf{x}, D)}{\partial \mathbf{x}^T} = \begin{bmatrix} 1 & 0 & \frac{\partial f_1(\mathbf{x})}{\partial \theta} & \frac{\partial f_1(\mathbf{x})}{\partial V} & \frac{\partial f_1(\mathbf{x})}{\partial \psi} \\ 0 & 1 & \frac{\partial f_2(\mathbf{x})}{\partial \theta} & \frac{\partial f_2(\mathbf{x})}{\partial V} & \frac{\partial f_2(\mathbf{x})}{\partial \psi} \\ 0 & 0 & 1 & \frac{\partial f_3(\mathbf{x})}{\partial V} & \frac{\partial f_3(\mathbf{x})}{\partial \psi} \\ 0 & 0 & 0 & 1 & 0 \\ 0 & 0 & 0 & 0 & 1 \end{bmatrix}, \quad \frac{\partial \mathbf{f}(\mathbf{x}, D)}{\partial D} = \left(\frac{\partial f_1(\mathbf{x})}{\partial D}, \frac{\partial f_2(\mathbf{x})}{\partial D}, \frac{\partial f_3(\mathbf{x})}{\partial D}, 0, 0 \right)^T. \tag{A1}$$

Let $q(\mathbf{x}) = V\Delta t \tan(\psi)/(2D)$ and $g(\mathbf{x}) = \theta + q(\mathbf{x})$. Then:

$$\frac{\partial f_1(\mathbf{x})}{\partial \theta} = V\Delta t \ \text{sinc}\,(q(\mathbf{x}))\sin\,(g(\mathbf{x})),$$

$$\frac{\partial f_1(\mathbf{x})}{\partial V} = \Delta t\ \mathrm{sinc}\ (q(\mathbf{x}))\cos\ (g(\mathbf{x})) - \Delta t\ q(\mathbf{x})\mathrm{sinc}\ (q(\mathbf{x}))\sin\ (g(\mathbf{x})) + \Delta t\ (\cos\ (q(\mathbf{x})) - \ \mathrm{sinc}\ (q(\mathbf{x})))\cos\ (g(\mathbf{x})),$$

$$\frac{\partial f_1(\mathbf{x})}{\partial \psi} = -\frac{V^2\Delta t^2}{2D}(1+\tan^2(\psi))\ \mathrm{sinc}\ (q(\mathbf{x}))\sin\ (g(\mathbf{x})) + \frac{V\Delta t\ (1+\tan^2(\psi))}{\tan(\psi)}\cos\ (g(\mathbf{x}))\cos\ (q(\mathbf{x}))$$
$$- \frac{V\Delta t\ (1+\tan^2(\psi))}{\tan(\psi)}\cos\ (g(\mathbf{x}))\ \mathrm{sinc}\ (q(\mathbf{x})),$$

$$\frac{\partial f_2(\mathbf{x})}{\partial \omega} = V\Delta t\ \mathrm{sinc}\ (q(\mathbf{x}))\cos\ (g(\mathbf{x})),$$

$$\frac{\partial f_2(\mathbf{x})}{\partial V} = \Delta t\ \mathrm{sinc}\ (q(\mathbf{x}))\sin\ (g(\mathbf{x})) + \Delta t\ q(\mathbf{x})\ \mathrm{sinc}\ (q(\mathbf{x}))\cos\ (g(\mathbf{x}))$$
$$+ \Delta t\ (\cos\ (q(\mathbf{x})) - \ \mathrm{sinc}\ (q(\mathbf{x})))\ \sin\ (g(\mathbf{x})),$$

$$\frac{\partial f_2(\mathbf{x})}{\partial \psi} = \frac{V^2\Delta t^2}{2D}\ (1+\tan^2(\psi))\ \mathrm{sinc}\ (q(\mathbf{x}))\cos\ (g(\mathbf{x})) + \frac{V\Delta t\ (1+\tan^2(\psi))}{\tan(\psi)}\sin\ (g(\mathbf{x}))\cos\ (q(\mathbf{x}))$$
$$- \frac{V\Delta t\ (1+\tan^2(\psi))}{\tan(\psi)}\sin\ (g(\mathbf{x}))\ \mathrm{sinc}\ (q(\mathbf{x})),$$

$$\frac{\partial f_3(\mathbf{x})}{\partial V} = \frac{\Delta t}{D}\tan(\psi),$$

$$\frac{\partial f_3(\mathbf{x})}{\partial \psi} = \frac{V\Delta t}{D}(1+\tan^2(\psi)),$$

$$\frac{\partial f_1(\mathbf{x})}{\partial D} = \frac{V\Delta t}{D}q(\mathbf{x})\ \mathrm{sinc}\ (q(\mathbf{x}))\ \ \sin\ (g(\mathbf{x})) - \frac{V\Delta t}{D}\cos\ (q(\mathbf{x}))\cos\ (g(\mathbf{x})) + \frac{V\Delta t}{D}\mathrm{sinc}\ (q(\mathbf{x}))\cos\ (g(\mathbf{x})),$$

$$\frac{\partial f_2(\mathbf{x})}{\partial D} = -\frac{V\Delta t}{D}q(\mathbf{x})\ \mathrm{sinc}\left(\frac{V\Delta t\ \tan(\psi)}{2\ D}\right)\cos\ (g(\mathbf{x})) - \frac{V\Delta t}{D}\cos\ (q(\mathbf{x})) + \frac{V\Delta t}{D}\ \mathrm{sinc}\ (q(\mathbf{x}))\ \ \sin\ (g(\mathbf{x})),$$

$$\frac{\partial f_3(\mathbf{x})}{\partial D} = -\frac{2q(\mathbf{x})}{D}.$$